

Review article: Performance assessment of radiation-based field sensors for monitoring the water equivalent of snow cover (SWE)

Alain Royer^{a,b,*}, Alexandre Roy^{b,c}, Sylvain Jutras^d, Alexandre Langlois^{a,b}

^aCentre d'Applications et de Recherche en Télédétection (CARTEL), Université de Sherbrooke, Sherbrooke, Québec, Canada

^bCentre d'études nordiques (CEN), Québec, Canada

^cDépartement des Sciences de l'Environnement, Université du Québec à Trois-Rivières, Trois-Rivières, Québec, Canada

^dDépartement des sciences du bois et de la forêt, Université Laval, Québec City, Québec, Canada

* Corresponding author

Abstract

Continuous and spatially distributed data of snow mass (water equivalent of snow cover, SWE) from automatic ground-based measurements are increasingly required for climate change studies and for hydrological applications (snow hydrological model improvement and data assimilation). We present and compare four new-generation sensors, now commercialized, that are non-invasive based on different radiations that interact with snowpack for SWE monitoring: Cosmic Ray Neutron Probe (CRNP); Gamma Ray Monitoring (GMON) scintillator; frequency-modulated continuous-wave radar (FMCW-Radar) at 24 GHz; and Global Navigation Satellite System (GNSS) receivers (GNSSr). All four techniques have relatively low power requirements, provide continuous and autonomous SWE measurements, and can be easily installed in remote areas. A performance assessment of their advantages, drawbacks and uncertainties are discussed from experimental comparisons and a literature review. Relative uncertainties are estimated to range between 9 and 15% when compared to manual in situ snow surveys that are also discussed. Results show: • CRNP can be operated in two modes of functioning: beneath the snow, it is the only system able to measure very deep snowpacks (> 2000 mm w.e.) with reasonable uncertainty across a wide range of measurements; CRNP placed above the snow allows SWE measurements over a large footprint (~20 ha) above a shallow snowpack; in both cases, CRNP needs ancillary atmospheric measurements for SWE retrieval. • GMON is the most mature instrument for snowpacks that are typically up to 800 mm w.e.; Both instruments, CRNP (above snow) and GMON, are sensitive to surface soil moisture. • FMCW-Radar needs auxiliary snow depth measurements for SWE retrieval and is not recommended for automatic SWE monitoring (limited to dry snow). FMCW-radar is very sensitive to wet snow, making it a very useful sensor for melt detection (e.g., wet avalanche forecasts); • GNSSr allows three key snowpack parameters to be estimated simultaneously: SWE (range: 0 - 1000 mm w.e.), snow depth and liquid water content, according to the retrieval algorithm that is used. Its

low cost, compactness and low mass suggest a strong potential for GNSSr application in remote areas.

Key word: Snow Water Equivalent, electromagnetic wave sensors, Cosmic Ray Neutron Probe, Gamma Ray Monitoring, frequency-modulated continuous-wave radar, Global Navigation Satellite System, sensor performance review

1. Introduction

Snow cover on the ground surface plays an important role in the climate system due to its high albedo, heat insulation that affects the ground thermal regime, and its contribution to snow runoff and soil moisture. Snow water equivalent (SWE, its mass per unit area) is expressed in kg m^{-2} , but also is commonly shown in units of mm of water equivalent, mm w.e. It is an Essential Climate Variable (ECV) for monitoring climate change, as recognized by the Global Climate Observing System (GCOS-WMO, 2016; <https://gcos.wmo.int/en/essential-climate-variables>), which aligns with the WMO-Global Cryosphere Watch Initiative (Key et al., 2016; <https://globalcryospherewatch.org>). SWE monitoring is also of primary importance for hydrological forecasting and preventing flooding risks over snowmelt-dominated basins in mountainous and cold climate regions. Snow station distributions are generally sparse in high latitude regions, remote areas and high mountains (Bormann et al., 2013; Key et al., 2015, 2016; Pirazzini et al., 2018; Heberkorn, 2019; Brown et al., 2019, 2021; Royer et al., 2021), given that monitoring is generally based upon expensive and occasional (weekly to monthly) manual sampling. Automation of SWE measurement networks is an essential medium-term prospect, especially since reliable and automatic instrument alternatives exist (Dong, 2018; this study).

Various in situ field devices and approaches for measuring the temporal dynamics of SWE are available, all of which have their strengths and limitations (see the review by Rasmussen et al., 2012; Kinar and Pomeroy, 2015; Pirazzini et al., 2018). Some are invasive (i.e., destroying the snowpack or changing its properties), while others that are based on different remotely sensed approaches are non-invasive. Here, we focus on a new generation of radiation-based field sensors that directly measure SWE, i.e., measuring a signal that is proportional to the snow mass per unit area. In this study, we do not consider sensors that are based on pressure and load cell sensors (snow pillows), snowmelt lysimeters, dielectric sensors (e.g., the SNOWPOWER system, commercially available as the Snowpack Analyzer) or acoustic sensors (see Kinar and Pomeroy, 2015). Neither do we consider indirect approaches, such as those based on snow-depth monitoring, combined with a model of snow density evolution (Yao et al., 2018). We also exclude satellite-based approaches.

The objective of this paper, therefore, is to present a performance review of four selected non-invasive sensors (Table 1), viz., the Cosmic Ray Neutron Probe (CRNP), the Gamma Ray Monitoring (GMON) scintillator, frequency-modulated continuous-wave radar (FMCW-Radar) and Global Navigation Satellite System (GNSS) receivers (GNSSr). All four

approaches have common features: easy to install; low power (e.g., powered by solar panels); provide continuous and autonomous SWE measurements; and deployable in remote areas. The continuous or quasi-continuous SWE measurement capability is defined here relative to the application, such as for seasonal SWE monitoring, for hydrological model validation, or to follow an event of a short winter storm. Surface-based radar scatterometers and microwave radiometers have not been considered in this study because 1) they are still in early stages of development or are currently not operational, and 2) they have heavy maintenance demands (not autonomous) and are still relatively expensive. These include, for example, scatterometers (Werner et al., 2010; Wiesmann et al., 2010; King et al., 2015; Werner et al., 2019), microwave radiometers (Langlois, 2015; Roy et al., 2016, 2017; Wiesmann et al., 2021); radar interferometers (Werner et al., 2010; Leinss et al., 2015; Pieraccini and Miccinesi, 2019; GPRI brochure, 2021), and Stepped-Frequency Continuous Wave Radar (SFCW) instruments (Alonso et al., 2021).

Sect. 2 provides background information on the basic principles of each of the four sensors that are presented in Table 1. Examples of SWE temporal series comparisons from four different instruments that were acquired in Québec, Eastern Canada, are given in Sect. 3.1 and 3.2: comparisons between EDF's CRNP (NRC sensor) and GMON on one hand, and GNSSr, FMCW-Radar and GMON on the other hand. This permits performance evaluations for each system, including uncertainty analysis, compared to manual SWE measurements. We complement these uncertainty assessments with a review of additional results from previous studies (Sect. 3.3, Table 2). Advantages and drawbacks of these sensors are then discussed in Sect. 4 (Table 3).

2. Radiation-based SWE sensor review

The main characteristics of the four reviewed sensors are summarized in Table 1, with the acronym that is used to denote them, together with their commercial names. There are two operation modes for the Cosmic Ray Neutron Probe (CRNP); thus, five cases were considered. All of these sensors allow quasi-continuous measurements throughout the winter without maintenance, and are powered by solar panels and batteries. The measuring principles of each of the instruments are illustrated in Fig. 1 and shown in Fig. 2. In this section, we only recall the main principles of functioning and the key elements of SWE retrieval, given that all sensors are well described in detail in the cited references.

Aspects that are related to the measurement scale of each sensor are critical to SWE measurements, since SWE is generally highly variable spatially, depending upon the ecosystem and terrain (Kinar and Pomeroy, 2015; Dong, 2018). These questions are discussed in Sect. 4.

Table 1. SWE sensors that were studied and acronyms that were used. FMCW: frequency-modulated continuous-wave radar; GNSS: Global Navigation Satellite System, including GPS (USA), GLONASS (Russia), Galileo (Europe) and Beidou (China) satellite constellations. The frequency (Freq.) of the electromagnetic (EM) wave that was used and their approximate maximum Snow Water Equivalent (SWE_{max}) measurement limit capabilities are given. SD: snow depth. See Fig. 1 for measurement principle conceptualization and Fig. 2 for photos.

Sensor	Acronym	Approach	Freq. GHz	SWE _{max} (mm)	Comments	Commercial Name	Main recent references
Cosmic Ray Neutron Probe	CRNP	Sensor beneath snowpack	-	up to 2000	Measures total snow, ice and water amount	SnowFox	https://hydroinnova.com
		Sensor above snowpack		~ 150-300		Hydroinnova CRS-1000/B	https://hydroinnova.com Bogena et al., 2020
						NRC EDF-Fr	Gottardi et al., 2013
						Cosmic Ray Detector (CRD)	Geonor Inc.
Gamma Ray scintillator	GMON	Sensor above snowpack	3.53 10 ¹¹ 6.31 10 ¹¹	up to 600 - 800	Measures total snow, ice and water amount	CS725 Campbell Sci.	Choquette et al., 2013 Smith et al., 2017 http://www.campbellsci.ca
Frequency-modulated continuous-wave Radar	FMCW-Radar	Active sensor above snowpack	24	~1000	Requires SD measurements Also measures stratigraphy	Sentire™ sR-1200 IMST Inc.	Pomerleau et al., 2020 https://shop.imst.de
Global Navigation Satellite System receivers	GNSSr	2 antennas above/ beneath snowpack	1.575 - 1.609	Up to 1500	Measures also Liquid Water Content and SD estimates	SnowSense	Henkel et al., 2019 Koch et al., 2020 https://www.vista-geo.de/en/snowsense/

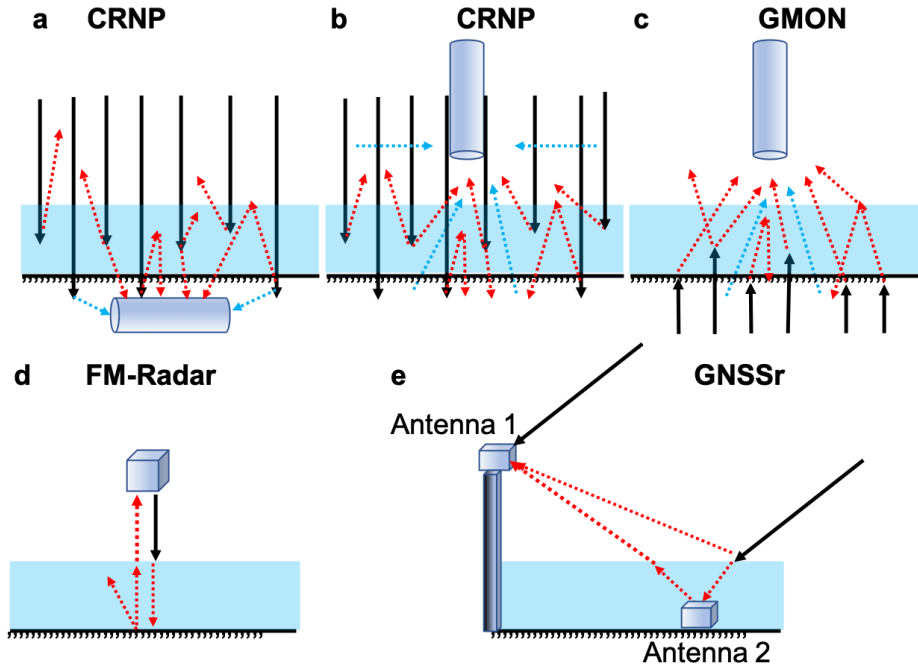


Figure 1 Diagram of radiation paths for the five approaches (see Table 1). In all figures, black arrows correspond to natural (a, b, c) or emitted (d, e) signals and dotted red arrows to rays interacting with snow (the lower the signal reaching the sensor, the higher the SWE). **a)** Cosmic Ray Neutron Probe (CRNP) below the snow, buried in the ground. In this case, black arrows are ambient neutrons generated primarily by interactions of secondary cosmic ray neutrons with terrestrial and atmospheric nuclei. Dotted red arrows are neutrons interacting with snow, which decrease when SWE increases. Dotted blue arrows are neutrons interacting with soil moisture. **b)** CRNP above the snow, looking downward. Same as (a) for the arrow meanings, but dotted blue arrows are neutrons interacting with soil and atmospheric moisture. **c)** Gamma Ray Monitor (GMON) sensor. Same as (a) for the arrow meanings. **d)** Frequency-modulated continuous-wave radar (FMCW-Radar) looking downward above the snow. Black arrow is the radar-emitted wave at 24 GHz. **e)** Global Navigation Satellite System (GNSS) receivers. The two antennas receive signals emitted by all of the GNSS satellites in the antennas' field of view and at all incidence angles: only one incident ray (black arrow) at one angle is shown. According to the inversion algorithm, different rays that interact with the snow (dotted red arrows) are used. For the SnowSense system, independent measurements at antenna 1 and antenna 2 are analyzed.

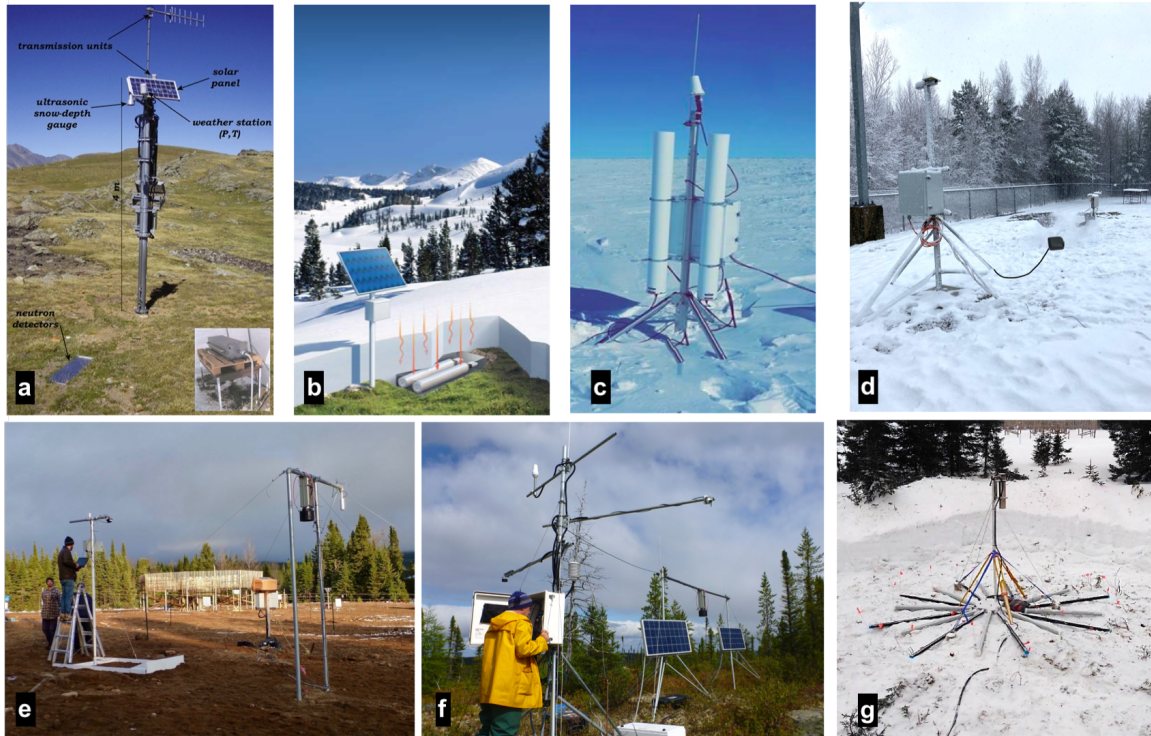


Figure 2. Photographs of sensors that were analyzed. **a)** Cosmic Ray Neutron Probe (CRNP) from the EDF French network (Nivomètre à Rayon Cosmic, NRC) at the Lac noir station in Ecrins-Pelvoux massif, France. One can see the neutron probe buried in the ground (also shown in inset) and the mast, which carries ancillary meteorological sensors. Credit: Delunel et al. (2014). **b)** SnowFox CRNP set at ground level beneath the snow cover. Similar to (a), the system requires measurements of atmospheric conditions. Credit: Hydroinnova SnowFox manual. **c)** Same sensor as in (b), but the Hydroinnova CRS-1000/B sensor is placed above the snow, measuring ambient and upward neutron counts, with the latter being attenuated by the snowpack. Crédit: Philip Marsh, Wilfrid Laurier University, Waterloo, ON, Canada; sensor in the tundra at Trail Valley Creek, Changing Cold Regions Network <http://ccrnetwork.ca>. **d)** GNSSr installed at the Université de Sherbrooke SIRENE site. The antenna that was placed on the ground (beneath the snow) was made visible at 3 m from the mast, on top of which a second antenna was affixed. Credits: Alain Royer. **e)** The FMCW-Radar (on the left) and the GMON (on the right) at the NEIGE-Forêt Montmorency site. A metallic plate on the ground in the field-of-view of the radar substantially increases radar echoes. In the background of photo (e), one can see the solid precipitation gauge, which is known as the Double Fence Intercomparison Reference (DFIR). Credits: Alain Royer. **f)** Meteorological and snow (GMON) automatic station at the LeMoyné James-Bay, Québec, Canada site in a sub-arctic environment (Prince et al., 2019). Credits: Alain Royer. **g)** The GMON at the NEIGE-Forêt Montmorency site set up to boost ^{40}K counts with pipes filled with potassium fertilizer. Credit: Sylvain Jutras.

2.1 Cosmic Ray Neutron probe (CRNP)

CRNP measurement is based on the moderation of ambient neutrons by hydrogen in water, snow and ice. The intensity of natural low-energy cosmic ray neutron emission is inversely correlated with the amount of hydrogen in the soil (Zreda et al. 2008; Andreasen et al., 2017) or snow cover (Desilets et al. 2010; Gottardi et al., 2013; Sigouin and Si, 2016; Gugerli et al., 2019; Bogena et al., 2020). Even though the principle of this approach has been known since the 1970s, it attained a level of operational maturity in the 2000s, especially with the use of commercialized soil moisture probes. Électricité de France (EDF)

183 successfully used a network of cosmic-ray probes (denoted Nivomètre à Rayon Cosmique,
184 NRC; this sensor is composed of two neutron detector tubes filled with Helium 3, ^3He)
185 that were buried under the snowpack to measure SWE for more than a decade in the
186 French Alps and in the Pyrenees (Fig. 2a, sensor placed at 3.5 m from a 6 m mast) (Paquet
187 and Laval, 2006; Paquet et al., 2008; Gottardi et al., 2013; Delunel et al., 2014).
188 Ephemeral, shallow snow cover across the UK is monitored by the COSMOS-UK network
189 of 46 sites equipped with the CRNP Hydroinnova CRS-2000 or CRS-1000/B models
190 (<https://cosmos.ceh.ac.uk>; Evans et al., 2016).

191
192 There are two experimental approaches for CRNP-based SWE monitoring (Fig. 1a,b): 1)
193 with the probe at the ground level beneath the snow (such as EDF' NRC, Fig. 2a, and the
194 SnowFox sensor for Hydroinnova, Fig. 2b), or 2) with the probe placed a few meters above
195 the snow surface (Fig. 1b), such as the one proposed by Hydroinnova (Fig. 2c) (CRS-
196 1000/B, Hydroinnova, Albuquerque, NM, USA; http://hydroinnova.com/snow_water.html). Using dual-channel, the system is composed of two detector tubes
197 filled with $^{10}\text{BF}_3$; one is sensitive to neutrons with a maximum energy of ~ 0.025 eV,
198 whereas the second is sensitive to moderated energy neutrons from ~ 0.2 eV to 100 keV.
199 The cosmic ray probe above the snowpack (Fig. 1b) is an attractive SWE measurement
200 tool because it can provide direct estimates of SWE within a 20 to 40 ha footprint (20 ha
201 corresponds to a circle of 252 m radius) (Desilets and Zerda, 2013; Schattan et al., 2017).
202 In contrast, the footprint of a probe that is installed under the snow is limited to a spot
203 measurement above the sensor (Fig. 1a). While approach (1a) permits measurements of
204 very thick snow cover (> 1000 mm SWE) (Gugerli et al., 2019), the drawback of approach
205 (1b) is that it is limited to low SWE measurements (typically < 150 mm SWE) over
206 homogeneous flat terrain. However, in the Austrian Alps, contrary to previous studies,
207 Schattan et al. (2017) claim not to have measured saturation for a snowpack of the order
208 of 600 mm SWE, over an estimated footprint with 230 m radius.

209
210
211 The CRNP method requires creating a function for converting neutron counts to snow
212 water equivalent (Paquet et al., 2008; Gottardi et al., 2013; Sigouin and Si, 2016;
213 Andreasen et al., 2017; Schattan et al., 2017; Delunel et al., 2014; Bogena et al., 2020).
214 Desilets (2017) provides the calibration procedure in detail. Neutron counts must be
215 accumulated over a specified period of time (e.g., from 6 h to 24 h). The CRNP method
216 requires that the counting rate must first be known (calibrated) and that disturbance
217 effects on measured cosmic rays at the site location have to be taken into account.
218 Disturbance effects that need to be corrected include temporal variations in the natural
219 cosmic-ray flux and variations in air pressure and atmospheric water vapor on site
220 measurements during the count time. Temporal variation in cosmic-ray flux can be
221 determined from the NMDB database (Real-Time Database for high-resolution Neutron
222 Monitor measurements; www.nmdb.eu), thereby providing access to reference neutron
223 monitor measurements from stations around the world. Corrections for air pressure
224 (linked to the altitude of the station) and atmospheric water vapor variations require
225 ancillary standard meteorological sensors, which measure atmospheric pressure, air
226 temperature and relative humidity.

While accuracy losses that are linked to atmospheric disturbances (pressure and humidity corrections) are relatively weak (a few percent), this is not the case for primary variations in the natural cosmic-ray flux (Andreasen et al., 2017), which may drastically change the results of SWE estimation. This flux can vary up to 30% over long periods (weeks to months), thereby causing errors up to 50% in SWE estimates when they are not considered (Paquet and Laval, 2006). Therefore, it is important to correct the measured signal using the closest world reference station in the vicinity of the measurement site. If not available, a second cosmic-ray sensor is required to produce accurate SWE estimates using normalized signals (above and beneath snow) as done by the Cosmic Ray Detector commercialized by Geonor Inc. (www.Geonor.com).

In the case of the second approach, where the probe is installed above the ground surface (Fig. 1b), the probe must be calibrated for soil moisture. If soil moisture correction is not applied on the winter signal measurements, retrieved SWE values will be systematically overestimated. This bias can be corrected using measurements of CRNP signal without snow, just prior to the onset of snow cover, or using soil moisture probe during the winter (see Sect. 4).

2.2 Gamma Ray scintillator (GMON)

Monitoring snow water equivalent by using natural soil radioactivity is a well-known approach (Bissell and Peck, 1973). Since 1980, an airborne snow survey program using this technology has successfully collected areal mean SWE data for operational flood forecasting over the whole of northwestern North America, including the Rocky Mountains, Alaska and Great Plains (National Operational Hydrologic Remote Sensing Center, <https://www.nohrsc.noaa.gov/snowsurvey/>). The mean areal SWE value is based on the difference between gamma radiation measurements over bare ground and snow-covered ground, the latter being attenuated by the snowpack (Carroll, 2001).

The principle of SWE measurements that are based on the Gamma Monitor (GMON) ray scintillator is the absorption by the water, regardless of its phase (liquid, snow or ice), of the natural radioactive emission of Potassium-40 (^{40}K) from soils (Ducharme et al., 2015). This naturally occurring radioactive isotope of potassium has a gamma emission of 1.46 MeV. The GMON probe also measures the emission of Thallium-208 (^{208}Tl), which emits gamma rays at a slightly higher energy (2.61 MeV) that originate from the decay of Thorium 232 (Choquette et al., 2013; Wright, 2013; Stranden et al., 2015). Both of these elements are common to almost all types of surfaces, regardless of whether these are organic or non-organic soils. However, we observed that the isotope associated with the higher count (i.e., ^{40}K) is generally the most reliable.

The GMON, which is manufactured by Campbell Scientific (Canada) (CS7525; <http://www.campbellsci.ca/cs725>), is composed of a tube 62 cm long, and 13 cm in diameter, weighing 9 kg. The experimental set-up, which is illustrated in Fig. 1c, is based on the initial, snow-free measurement of the number of counts for ^{40}K or ^{208}Tl per period

of time, which would be later decreased by the presence of the snowpack. Typically, 300 000 and 60 000 counts per 24 hours for ^{40}K and ^{208}Tl , respectively, are suggested as minimal values to provide accurate SWE measurements (CS725 Snow Water Equivalent Instruction Manual, 2017, Campbell Scientific [Canada] Corporation, Edmonton, AB; https://s.campbellsci.com/documents/ca/manuals/cs725_man.pdf). The observed rate of soil emission at each site allows the operator to define the minimum sampling time frequency. Seeding experiments conducted using potassium fertilizer show the potential for increasing potassium counts that are measured by the CS725 by up to 80% at sites where low counts are found (Wright et al., 2011). As is the case for ground-pointing CRNP, measuring the base-line signal of the radiation energy emanating from the ground prior to the first snowfall is a critical step in signal processing, given that it also depends upon soil moisture (SM) during the winter and spring periods. SM attenuates the natural dry-ground emission, resulting in an overestimate of SWE during signal processing when SM increases (Choquette et al., 2013) (see Sect. 4).

The CS725-Campbell GMON sensor has been the subject of a detailed performance analysis within the framework of the WMO Solid Precipitation Intercomparison Experiment (Smith et al., 2017). Moreover, since the device is sensitive to water contained in soils, it can be successfully used to estimate soil moisture during snow-free seasons. An operational GMON network, with a sampling frequency of 6 h, is actually deployed across the southern part of Québec and Labrador, northeastern Canada (45-55°N); it accounts for 116 stations that are operated by Hydro-Québec (87), Rio-Tinto (13), Ministère de l'Environnement et de la Lutte contre les changements climatiques of the Québec Government (10), Parks Canada (4), and the Government of Newfoundland and Labrador (2), and which are dedicated to water resource forecasting (Alexandre Vidal, Hydro-Québec, personal communication, November 2020). Also, these continuous measurements from the GMON Quebec network are demonstrably very useful for validating the assimilation of microwave observations into a snow model (Larue et al., 2018). Recently, GMON had also demonstrated its robustness in a research project on seasonal snow monitoring from a station that was installed at 4962 m asl in the Nepalese Himalayas (Langtang Valley) to quantify the evolution of SWE (Kirkham et al., 2019).

2.3 FMCW radar (FMCW-Radar)

The principle of frequency-modulated continuous-wave (FMCW) radar has been well known since the 1970s (see the reviews by Peng and Li, 2019 and by Pomerleau et al., 2020) and has been popularized for snow studies since Koh et al. (1996), Marshall et al. (2005), and Marshall and Koh (2008), among others, were published. FMCW-Radar is an active system design for distance measurements. The radar emits a wave at variable frequencies that are centered on a reference frequency. When the radar receives a return from a target, the frequency difference between the emitted and reflected signals is measured (Fig. 1d). Since the frequency change rate is known, the time between the emission and the reception of the echo can be measured, from which the radar-target distance is calculated.

The principle of SWE retrieval is based on the time measurement of wave propagation in the snowpack that is proportional to the snow refractive index (square of permittivity), which changes the wave-speed propagation. As the refractive index of snow can be linked to its density (Tiuri et al., 1984; Matzler, 1996; Pomerleau et al., 2020), SWE can be retrieved knowing the snow depth. The experimental set-up is shown in Fig. 1d and illustrated in Fig. 2e.

Two main FMCW-radar specifications are required for SWE measurement: the radar central frequency and its bandwidth that is scanned. The central frequency specifies three parameters: a) the loss in signal strength of an electromagnetic wave that would result from a line-of-sight path through free space (the higher the frequency, the greater the loss); b) its penetration depth (the higher the frequency, the less penetration power it has); and c) its sensitivity to liquid water content in the snowpack. The bandwidth specifies the distance resolution and, thus, the precision: the wider the bandwidth, the lower the resolution. There is negligible frequency dependency of the snow refractive index (n'), which governs wave propagation in the snowpack. The refractive index (n') is linked to snow density (ρ) by a linear relationship: $n' = 8.6148 \cdot 10^{-04} \rho + 9.7949 \cdot 10^{-01}$ (Pomerleau et al., 2020).

For snow studies, several FMCW radars with different frequencies and resolutions are used, such as those common at the X-band (10 GHz), operating over 8–12 GHz (Ellerbruch and Boyne, 1980; Marshall and Koh, 2008). They provide a vertical resolution on the order of 3 cm. In contrast, L-Band FMCW radar (1.12–1.76 GHz) allows greater penetration but suffers from reduced vertical resolution (Yankielun et al., 2004). Multiband band FMCW radars have also been developed (Rodriguez-Morales et al., 2014), such as an L/C-band (2–8 GHz) that was used to successfully retrieve snow depth (Fujino et al., 1985), a C/Ku (8–18 GHz) large wideband FMCW radar that is capable of detecting crusts as thin as 0.2 mm within the snowpack (Marshall and Koh, 2005), or the improved (C-, X-, and Ka-band) radar (Koh et al., 1996). Operating frequencies of commercial, low-cost radar systems, such as those that are adopted for automotive radar systems (Schneider, 2005), are now available for K-band (24 GHz) and W-band (77 GHz) applications.

The availability of such new types of lightweight and very compact 24-GHz FMCW radar systems has motivated our research group to assess their ability to monitor the SWE continuously and autonomously (Fig. 2e) (Pomerleau et al., 2020). The FMCW-Radar that is used, which is centered on 24 GHz (K-band), is manufactured by IMST (IMST sentire™, IMST, Kamp-Lintfort, Germany; <http://www.radar-sensor.com/>); its housing module is very compact (114.0 mm × 87.0 mm × 42.5 mm) and weighs 280 g. This FMCW-Radar has a bandwidth of 2.5 GHz, scanning over 23–25.5 GHz, which provides a resolution of 6 cm in the air. These specifications appear to be a good compromise between penetration and resolution capabilities for SWE estimation, while keeping the sensor affordable, light and compact, with low power consumption. The radar penetration depth (δPr) of dry snow significantly decreases with density following a power law, which varies with temperature (see Fig. A2, Pomerleau et al., 2020). At $T = 0^\circ\text{C}$, δPr decreases from 6.78 to 4.81, 3.26

and 2.05 m for respective snow densities of 150, 200, 275 and 400 kg m⁻³ (Pomerleau et al., 2020). Wet snow drastically reduces δPr , given that liquid water strongly absorbs the radar signal, leading to high reflectivity at the air/wet snow interface and weak transmissivity. For example, the two-way radar penetration depth decreases abruptly from 2 m for dry snow at a density of 400 kg m⁻³ to 0.05 m for wet snow with 0.5% of liquid water content (as a volume fraction). It should be noted that this strong sensitivity to wet snow allows the radar to precisely detect the onset of snowpack surface melt, a benefit that is discussed in Sect. 4.

One of the main interests of this approach is its potential capacity to estimate SWE from a small remotely piloted aircraft (RPA). Over the Arctic, snow cover can generally be characterized as a two-layer snowpack structure, which is composed of a dense wind-slab layer overlaying a less-dense hoar at depth (Rutter et al., 2019; Royer et al., 2021). Thus, assumptions can be made regarding the mean refractive index of each of these layers, thereby allowing SWE to be estimated (Kramer et al., 2021). Hu et al. (2019) also showed the usefulness of imaging FMCW synthetic aperture radar onboard the RPA. Several studies have also shown the potential of FMCW radar for different applications, such as avalanche studies (Vriend et al., 2013; Okorn et al., 2014; Laliberté et al., 2021), snow stratigraphy based on successive FMCW echo analyses (Marshall and Koh, 2005; Marshall et al., 2007), snowpack tomography (Xu et al., 2018), and ice thickness monitoring (Yankielun et al., 1993; Gunn et al., 2015). Pomerleau et al. (2020) obtained highly accurate measurements of lake ice thickness using the 24 GHz FMCW radar, with a root-mean-square difference (RMSD) of 2 cm accuracy up to ≈ 1 m ice thickness (derived from 35 manual in situ measurements).

2.4 GNSS receivers (GNSSr)

The principle of SWE retrieval based on Global Navigation Satellite System (GNSS) receivers is to use the signals that are emitted at 1.575 and 1.609 GHz. by the GNSS satellite constellations. SWE can be related to the carrier phase change that is induced by the delay caused by the snowpack at ground level. With two static receivers (standard GNSS antennas), i.e., one placed under the snow and the other above the snow, carrier phase measurements of both receivers can be compared and SWE derived using the onboard measurement hardware (Fig. 1e) (Henkel et al., 2018). Comparing GNSS signal attenuation measurements between the two antennas (below and above the snowpack) also permits the retrieval of Liquid Water Content (LWC) of the wet snow (Koch et al., 2019). Snow depth retrieval has been operational for longer, based on interferometric reflectometry of GNSS signals (see Larson et al. 2009; Larson, 2016). Steiner et al. (2019) used a slightly simplified retrieval algorithm based on the path delay estimates of the GPS signals while propagating through the snow cover due to both refraction at the air-snow interface and decrease in wave velocity in the medium.

This relatively recent and novel approach has been validated (Henkel et al., 2018; Steiner et al., 2018; Koch et al., 2019; and Appel et al., 2020). A system has now been commercialized by VISTA Remote Sensing in Geosciences GmbH, Munich, Germany

(SnowSense®, <https://www.vista-geo.de/en/snowsense/>). The experimental set-up is described in Fig. 1e, based on a low cost and lightweight system. In this study, we used the SnowSense system for monitoring SWE and LWC throughout a winter, together with other sensors (see Results Sect. 3). We also developed our own system, shown in Fig. 2d.

Another promising way to monitor SWE, which is based on the same principle of GNSS, is the use of powerful satellite transmissions as illumination sources for bistatic radar. This so-called “Signals-of-opportunity (SoOp)” approach covers a wide range of frequencies, such as emissions from United States Navy Ultra High Frequency (UHF) Follow-On (UFO) communication satellites in P-Band frequencies (between 240-270 MHz). From two P-band antennas (one direct and one reflected), Shah et al. (2017) demonstrated the feasibility of retrieving SWE using the phase change in reflected waveforms, which is linearly related to the change in SWE. These methods were not included in this review since they are still in the development stage and not sufficiently mature to be operational.

3. Results

Continuous and simultaneous recordings of different instruments on different sites were analyzed to evaluate their behavior in terms of their temporal evolution. Manual measurements were used to compare the data between them. First (Sect. 3.1 and 3.2), two experiments we conducted were compared: GMON and CRNP (Sect. 3.2.1); and GMON, Radar and GNSSr (Sect.3.2.2). A comprehensive literature review and evaluations of similar sensors are then presented in Sect. 3.3. This later section also includes uncertainty estimates of our experiments and from this review, which are synthesized in Table 2.

3.1 Experimental sites and methods

We compared four instruments at two snow research stations that were located in Québec (Canada). The first was the SIRENE site (Site Interdisciplinaire de Recherche en ENvironnement Extérieur), which is situated on the main campus of the Université de Sherbrooke in a temperate forest environment (45.37°N, -71.92°W, 250 m asl) (Fig. 2d). The second site is the NEIGE-Forêt Montmorency (NEIGE-FM) research station. The instruments were located in an open area (Fig. 2e) of the Montmorency experimental forest (47.32° N; -71.15° W, 640 m asl) of Université Laval (Quebec City), which is in the boreal forest. The NEIGE-FM snow research station is part of the World Meteorological Organization (WMO) Global Cryosphere Watch (GCW) Surface Network CryoNet (<http://globalcryospherewatch.org/cryonet/sitepage.php?surveyid=191>).

Two methods were used to obtain in situ manual SWE measurements in the vicinity of the four SWE-systems: the snowpit (SP) approach; and snow-tube core samplers (see Kinar and Pomeroy, 2015; López-Moreno et al., 2020). The SP-based SWE values (in mm = kg m⁻²) were derived from vertical continuous density profiles, which were determined by weighing snow samples at a vertical resolution of 5 cm (height of the density cutter). Assuming an accuracy of density cutter measurements of about 9% (Proksch et al., 2016),

the mean relative SWE accuracy from snowpit can be estimated to be of 6–12%. SWE estimates were also obtained by weighing the extracted core sample of known diameter (\emptyset) and snow depth using a coring tube. In this study, the core sampling was performed using three different snow tube models, which were averaged: “Carpenter” (Federal standard sampler, 3.7 cm \emptyset tube), the Hydro-Quebec snow tube (12.07 cm \emptyset), and an in-house Université Laval snow tube (15.24 cm \emptyset). The uncertainties of tube core sampling that we carried out on snowpack up to 600 mm SWE with large tubes is on the order of 6%, but can be higher, up to 12%. Such uncertainty is difficult to define, as discussed in Sect. 3.3 and in discussion contained in the Appendix. Furthermore, as manual measurements cannot be taken at the same location throughout a given winter period, this could generate uncertainty when compared to a fixed instrument, due to small-scale spatial variability of SWE and surface roughness (López-Moreno et al., 2020).

The snowpack properties were derived from GMON and CRNP systems throughout the entire winter season of 2008-2009 (Fig. 3) and from GMON, FMCW-Radar and GNSSr systems in 2017-2018 (Fig. 4). The CRNP probe that was used was the same as the French EDF probe that was placed on the ground (Paquet et al., 2008) and installed at about 5 m distance from the GMON footprint. The GMON was installed on a 2 m mast above the surface, located in a slight depression in comparison with the terrain where the CRNP was buried. The CRNP counts were accumulated over 1 hour and normalized against an identical probe that was installed nearby, just above the snow surface. The GMON counts were accumulated over 6 hours, and only ^{40}K counts were considered (TI counts were similar, but not shown). The GMON sensor was adjusted to take into account the soil moisture prior to snowfall accumulation, but not afterwards.

In addition to SWE measurements, continuous automatic snow depth measurements were performed using an ultrasonic ranging sensor (Campbell Scientific, SR50AT-L), and manually with a graduated probe around the sampling sites. LWC measurements were derived from GNSSr (Fig. 4). Air temperature (T) at 2 m height and total daily precipitation (tipping bucket rain gauge) were recorded at the SIRENE site; a threshold of $T = 0^\circ\text{C}$ was used to separate solid and liquid phases.

In this section, we present comparisons between these sensors with manual snowpit validation data that were measured as close as possible to the automatic instruments. The uncertainty of measurements, including other measurements that we carried out (not shown), is reported in Table 2.

3.2 Validation of measurements

3.2.1 Comparison of GMON- and CRNP-derived SWE seasonal evolution

Figure 3 shows the SWE evolution of a shallow snowpack (maximum snow depth of 56 cm) at the SIRENE site that was derived from daily mean values of the GMON and CRNP data throughout the winter season of 2008-2009.

Results show that GMON and CRNP evolve similarly over the winter, with GMON SWE being slightly higher after the first winter month ($\text{SWE} > 50 \text{ mm}$). This difference occurred

after a pronounced melting spell (29-30 December 2008) and is explained by the water that has accumulated on the ground under the GMON and not on the CRNP, due to the local terrain configuration. The moisture beneath the GMON formed a significant ice layer that lasted all winter. As this ice layer was not present in snowpits (the amount of water in an ice crust being otherwise difficult to measure), this could possibly explain differences between GMON and manual measurements. Precipitation (snowfall and rain) is also plotted, showing how GMON and CRNP develop with each event. For that given winter, rain-on-snow events were frequent, leading to moisture accumulation on the ground. Note also that at the end of the winter, there was ice that had not yet melted and water accumulation under the GMON, leading to a significant GMON overestimation in terms of snow w.e. but not in terms of total water. There was no more snow on the ground after 20 March 2009. The accuracy measurements are discussed in Sect. 4.2.

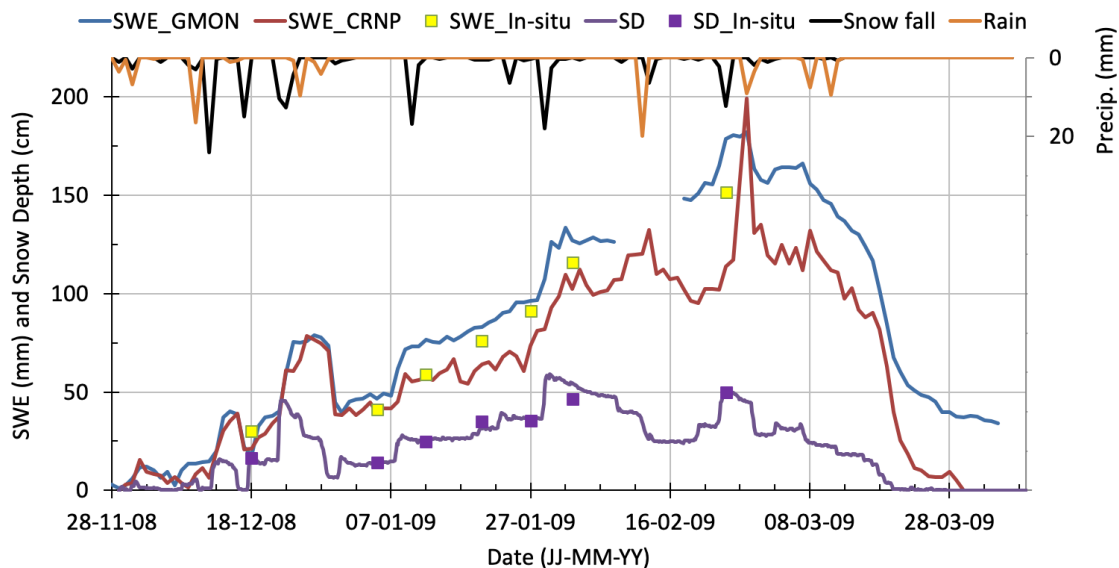


Figure 3. GMON- and CRNP-derived snow water equivalent (SWE, mm), snow depth (SD, cm), and recorded daily solid and liquid precipitation (Precip., mm, right hand scale), in comparison to validation data (in situ) at the SIRENE site for the winter season of 2008-2009. Continuous SD measurements (purple line) are from SR-50 and SD_in situ measurements (purple square) are from snowpits. Open yellow squares correspond to manual in situ SWE measurements.

3.2.2 Comparison of GMON-, Radar- and GNSSr-derived SWE seasonal evolution

Figure 4 shows the SWE evolution that was measured by the three instruments: GMON (^{40}K counts only), FMCW-Radar and GNSSr, which had been placed in close proximity to one another at the NEIGE-FM research station for the winter season of 2017-2018. A maximum snow depth of 120 cm was measured during the season, corresponding to 500 mm SWE maximum at the end of April.

The three instruments were compared to manual in situ measurements that had been derived from SP (red squares) and core (red triangles) approaches in Fig. 4. We

distinguished the two methods (SP and snow core) because they exhibit significant differences, with a RMSD of 33 mm (12%). These discrepancies are the result of two problems: 1) SWE spatial variability, mainly due to snow depth variability (López-Moreno et al., 2020); and 2) the method that was used, since the design of snow tubes and cutters has some influence on sampling errors and bias (Goodison et al., 1987). Therefore, uncertainty analyses (Sect. 3.3) were performed considering manual SP as the reference because the SP approach was used for both experiments.

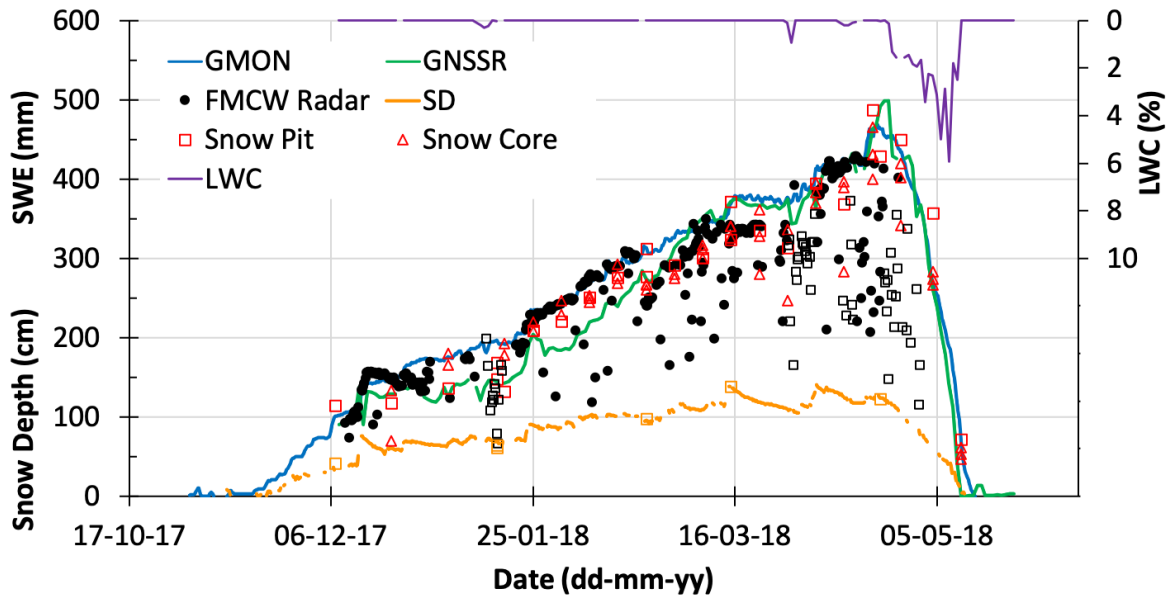


Figure 4. GMON- (blue line), FMCW Radar- (black closed circles) and GNSSr-derived (green line) snow water equivalent (SWE, mm), snow depth (orange line for SR50AT-L data and orange open squares for in situ data) (SD, cm) and GNSSr-derived Liquid Water Content (LWC, % volumetric, purple line, right scale), in comparison to in situ snowpit (open red square) and snow core (open red triangle) SWE measurements at the NEIGE-FM site for the winter season of 2017-2018. For FMCW-Radar data (in black), plain circles are for dry snow, while open squares correspond to wet snow.

The continuous simultaneous recordings from the different instruments permit temporal evolution analysis (Fig. 4). During the accumulation period, GMON shows relatively smooth and consistent evolution in SWE leading to a maximum of 465 mm on 19 April 2018, while the FMCW-Radar time series is more erratic and requires filtering to remove low SWE outliers. These points are mainly due to incorrect detection of the peak of the radar echo on the ground (snow-ground interface), sometimes with low amplitude, and which can be filtered with improved data quality processing of raw recording (Pomerleau et al., 2020). In particular, all data that were acquired under wet snow conditions (open black squares, Fig. 4), which correspond to melting periods with measured air temperature above 0° C, are obviously underestimated as expected, because of radar wave absorption by liquid water in the snowpack. Compared to the GMON, the GNSSr

signal increases with values that are lower than the GMON until mid-March at which point it continues to evolve with similar values, as the GMON SWE_{max} of 499 mm w.e. was reached on 23 April 2018. The behavior of the three instruments, showing different patterns of snow evolution, always remains close to in situ observations (RMSE compared to the snowpit for GMON and GNSSr are respectively 34 mm and 32 mm; Table 2). It should be noted that in Fig. 4, there is a small difference (+4 days) between the disappearance of snow cover that was recorded with GNSSr (11 May 2018) compared to GMON (14 May 2018). The GNSSr sensor is not sensitive to soil moisture, while GMON is, despite the instruments being located on a well-drained sandy site (NEIGE-FM site). In the case shown here, the end of snowmelt is well captured by both instruments. The accuracy between instruments is analyzed in Sect. 3.4, including a second winter season of continuous measurements at the NEIGE-FM site (2016-2017, Pomerleau et al., 2020).

GNSSr also measures the Liquid Water Content (LWC) of snow (purple line in Fig. 4). The non-zero LWC values correspond well to positive air temperatures that were recorded at this site, and also to the drop in FM-Radar measurements (open black squares).

3.3 Analysis of measurement uncertainty

It is challenging to compare the accuracy of several instruments, given that there is no absolute reference for estimating SWE (see Kinar and Pomeroy, 2015). In situ manual measurements are themselves subject to error, with varying precision depending upon the method that is being used. Errors are incurred that depend upon the types of density cutter, tube diameter, sampling quality that is operator dependent, and ice lenses in the snowpack, among other sources. This is a long-debated topic, with no actual established international standard protocol (Work et al., 1965; Goodison et al., 1981, 1987; Kinar and Pomeroy, 2015, López-Moreno et al., 2020). Commonly, the relative uncertainty for SWE measurement using snow core varies from 6% for shallow snowpack (0-300 mm w.e.), to 8% (300 – 1000 mm w.e.) for medium snowpack to 10-12 % for deeper snowpack (> 1000 mm w.e.) (see discussion in supplementary data). Moreover, because manual measurements cannot be taken at the same location during a given winter period, uncertainty can be introduced by well-known local spatial variability of snow depth that can occur at fine scales around the sensors. Such variability depends upon several factors, such as the region and the environment (Arctic area, aspect and slope in mountainous areas, for example), the micro-topography and roughness, the vegetation, and snow redistribution by the wind (Clark et al., 2011; Bormann et al., 2013; Rutter et al., 2014; Meloche et al., 2021; Royer et al., 2021). Furthermore, temporal variability of snowpack snow depth and SWE during the winter requires regular validation measurements throughout the season.

The sensor uncertainties were evaluated from results of our experiments (Sect. 3.2) and from published studies at other experimental comparison sites (this section). These other sites are: the Weissfluhjoch high-alpine site near Davos, Switzerland (46.83° N, 9.81° E, 2 536 m asl); Sodankylä, Finland (67.37° N, 26.63° E, 185 m asl); Caribou Creek, SK, Canada (53.95° N, -104.65°W, 519 m asl); and Fortress Mountain ski area, Kananaskis Country, Canadian Rocky Mountains, AB (50.82° N, -115.20° W, 2 330 m asl). We also conducted a

series of manual FMCW-radar measurements (e.g., instrument operated by hand, rather than automatically) over dry snowpack and compared them with in situ SWE measurements over a wide range of conditions (snow depth and density) in boreal forest (47° N, 18 points), subarctic taiga (54–56° N, 32 points) and Arctic tundra (69° N, 28 points) environments along a northeastern Canadian transect (Pomerleau et al., 2020).

Note that we only consider here the differences between instruments in the field and do not address accuracies that were derived from instrument calibration by the manufacturer.

Table 2 summarizes the uncertainties of each instrument and protocol (five cases: CRNP in and above ground, GMON, FMCW-Radar and GNSSr) in relation to in situ manual measurements (snowpit method), as well as against snow pillow and snow scale data that were considered as reference measurements by the authors of the publications consulted. The results from the COSMOS-UK network (Wallbank et al., 2021) were not included in the overall uncertainty analysis, because, in this study, depth-based SWE estimate of fresh snow was used to assess the uncertainty of CRNP (R^2 of 0.53, in the range of 0–40 mm w.e.). Moreover, soil moisture is usually high and variable in UK, which acts to increase uncertainties in the SWE estimate (Wallbank et al., 2021).

Even if the mechanical method is well known and has been proven over many years, the snow pillow can sometimes generate large errors when bridging processes occur that are linked to freeze–thaw cycles leading to disconnection of the weighing mechanism of the overlying snowpack and the surrounding snowpack (Kinar and Pomeroy, 2015). However, to compare measurements at a daily scale, they are worth looking at. In Table 2, the uncertainty that relates to the characterization of measurement dispersion compared to a reference was defined, when known. We used the root-mean-square difference (RMSD) between an instrument and a given reference, and by a linear regression over the whole range of measured SWE data that was defined by the coefficient of determination (R^2), the slope and the intercept. The number of points is also given.

Table 2 here

Uncertainty analysis does not allow us to determine the “best” instrument, due to the diversity of experimental conditions, including the range of SWE, the number of experimental sites and point measurements, and the analyses that are performed over one or several seasons. It appears that all five methods show a RMSD in the range of 14 to 48 mm (mean 33 ± 11 mm) against in situ snowpit manual measurements (Table 2). This represents a relative value of around 12% on average, depending on the instruments. The mean coefficient of determination for the linear regression is also substantially high (mean $R^2 = 0.92 \pm 0.07$). Calculated average slope is 0.976 ± 0.13 , meaning that in general, the instruments slightly underestimate SWE for higher SWE values compared to in situ measurements, even if this is not always the case (Table 2). RMSD increases slightly when the analysis was performed over a deep snowpack (0–1000 mm w.e.) and decreases when compared to another continuous instrument instead of manual data (instrument vs GMON and instrument vs snow pillow, average RMSD = 23 ± 10 mm, Table 2).

For the GNSSr instrument that allows the operator to differentiate dry from wet snow, Koch et al. (2020) have shown that SWE RMSD is about 2.4-fold higher for wet snow than for dry snow. They did not provide information on LWC uncertainty. In late winter 2021, for very wet melting snow, we did a validation measurement using the WISE A2 Photonic probe (snow liquid-water content sensor that is based on snow microwave permittivity measurements; <https://a2photonicsensors.com/wise/>). The GNSSr LWC was of 0.44 % (in volume) (the retrieved GNSSr SWE was 149 mm w.e) and the LWC from the in situ probe was of 0.47 % for the upper half of the snowpack. The snowpack SWE that was measured manually was 133 mm. The lower half of the snowpack was saturated with water. The uncertainty in wet SWE retrieval could result from approximations in the retrieval algorithm that is used. For example, the wet snow refractive index varies linearly with LWC, with a slope significantly dependent of the snow density (see the appendix of Pomerleau et al., 2020). This aspect could probably be addressed further by improved inversion.

The uncertainty comparison in Table 2 must be weighted according to the analysis conditions. The accuracy estimates can actually depend upon the number of points being used and their distribution over time. High inter-annual variability of the snowpack state (see Bormann et al., 2013; Lejeune et al., 2019) ideally would necessitate several years of measurements over the winter. The uncertainties of each GMON and CRNP instrument were derived from huge data sets that were based on operational networks from the GMON Hydro-Quebec network in Canada and the Alps' EDF network for the CRNP, respectively, with a very large number of samples taken over several years of experiments and from multiple sites. The accuracy of the GMON that is given by the manufacturer is ± 15 mm for SWE < 300 mm and $\pm 15\%$ for SWE of 300-600 mm, which is probably rather conservative. When SWE reference data and site adjustment process are well done, the GMON is able to report SWE with an error as low as 5% (Wright, 2011; Choquette et al., 2013; Wright et al., 2013). The accuracy of the SnowFox sensor (CRNP) that has been provided by the manufacturer (5-10%) must be confirmed. The GNSSr approach has recently been the subject of two different comparative analyses showing very promising results (Henkel et al., 2018; Koch et al., 2019), which were confirmed by our own results. Over a full season, we obtained an excellent relationship between GNSSr and in situ manual measurements (relative RSMD = 11%, Table 2) and compared with GMON (RMSD = 34 mm, 12%, $SWE_{GNSSr} = 1.126 SWE_{GMON} - 59.3$, $R^2 = 0.97$, 153 days).

4. Strengths and Weaknesses of Instruments

In this section, we review the advantages and drawbacks of each of the instruments that are presented, summarized in Table 3. This analysis is based on our experience on instruments and their performances, and a literature review on experimental results of measurements that were carried out with the same approaches. We only consider these field sensors for SWE measurements in terms of their continuous and autonomous capacities, from the perspective of an operational networking context, including criteria

regarding low maintenance and relatively easy installation without requiring heavy infrastructure. The four instruments that we analyzed are: CRNP with two experimental setups, i.e., instrument in the ground and above the snow; GMON; 24-GHz FMCW-Radar; and GNSSr (see Table 1 for acronyms and Fig. 1 for the experimental setup). They are all capable of working on batteries and solar panels, by adjusting, if necessary in certain cases, the measurement protocol, i.e. by reducing the frequency of acquisition and on-board data processing. Ten criteria were considered (Table 3): - the SWEmax capability; - other measured parameters; - whether ancillary data were required for SWE retrieval; - the temporal sampling rate, i.e., whether they were capable of quasi-continuous SWE measurement capability, although the notion of continuous SWE measurements is relative to the application; - the footprint of the sensor, i.e. taken here in the sense of the area from which emanates the measured radiation having interacted with the snow; - the power consumption; - the main strength of the approach; - their critical drawbacks; - the price of the instrument itself, knowing that the cost of the system may vary in case additional instruments are required for the SWE measurements. Also, the cost that is associated with on-site maintenance during winter should be considered here, but in our case, the 4 instruments are considered on the same basis, i.e., autonomous, with no need for intervention; - and the possibility of other applications.

The cost criterion is a very relative argument, which can influence the choice of decision-makers or researchers, depending upon the intended application (e.g., large network, in remote areas, among others) and also on the purchasers.

Table 3 here

To complement the main criteria that are presented in Table 3, we include the following additional considerations, which are reported in the literature, by order of presentation rather than order of merit.

The CRNP approach is based on neutron component that has absorption mean free path about an order of magnitude larger than that for gamma radiation. This makes it the most efficient system for very deep snowpack analysis (Paquet et al. 2008). Measurements over a snowpack of up to 2000 mm SWE were performed using the SnowFox sensor at the UC Berkeley Central Sierra Snow Lab in Soda Springs, CA (2 120 m asl; <https://vcresearch.berkeley.edu/research-unit/central-sierra-snow-lab>).

Regarding CRNP above the snow, Schattan et al. (2017) estimated the theoretical winter footprint over snow, which they defined as the distance from where neutrons originate. They found that 86%, 63% and 50% of neutrons originate within respective distances of 273, 102, and 49 m. In practice, the authors found that the average footprint during the season, based on measurements over almost three snow seasons, was estimated to be around 230 m, possibly more.

Moreover, CRNP is inherently weakly sensitive to interference from vegetation compared to systems that are based on EM low frequencies (GMON, FMCW-Radar and GNSSr). This is in part because the attenuation coefficient for fast neutrons ($\sim 0.01 \text{ m}^{-2} \text{ kg}$ in water, Murray and Holbert, 2020) is an order of magnitude smaller than the analogous attenuation coefficient in vegetation for GNSS microwaves (1.5 GHz) (e.g., Wigneron et al., 2017). Also, vegetation can itself be a significant source of electromagnetic emissions (Larson et al., 2014; Wigneron et al., 2017). The CRNP is affected by all sources of hydrogen within its measurement footprint. As Biomass increases the hydrogen concentration in the CRNP's footprint, it is possible to monitor changes in biomass (Vather et al., 2020).

The instruments pointing toward the soil, CRNP and GMON above the surface, are sensitive to soil moisture. This can be a relatively large source of error with these measurement principles, given that these sensors are interpreting near-surface soil liquid content as SWE. This is especially the case during spring freshets and mid-season thaw cycles (see Fig. 3 and Smith et al., 2017). Heavy rainfall on snow also leads to erroneous SWE estimates due to the occurrence of water ponding beneath the snow (Fig. 3). Installation on well-drained soils can mitigate these effects, as shown in Fig. 4. By assuming that soil moisture levels remain stable throughout winter, which can be the case when soil remains frozen (see Gray et al., 1985, 2011), this soil moisture-induced bias can be adjusted prior to the first snowfall or one must apply a correction based on soil moisture conditions that are otherwise known. Based upon 10+ years of experience with a large GMON network that is deployed in Quebec, Canada, over northern organic boreal soil, it has been shown that in most cases, SM does not vary substantially during the winter season (Choquette et al., 2013; Ducharme et al., 2015). To consider SM as constant, mathematical equations that are used in calculating SWE can be simplified. If the goal is to measure the total water that is available for hydrological purpose, this aspect can become an advantage.

Counter-based sensors such as CRNP and GMON need to accumulate enough counts for reliable SWE estimates. Thus, it may be necessary to accumulate the counts over an adjusted period of time (several hours, depending on the case), so that the measurement is not strictly continuous. This can prevent accurate detection of short events, sudden heavy snowfalls, for example.

For the GMON, depending on the type of soil at the measurement site, gamma ray emissions may not be sufficient and could require a longer integration period, as is the case for sites with thick organic soil layers. It is possible to enrich gamma emissions by using bags or pipes of potassium-rich fertilizer, thereby maintaining a shorter integration time. Wright et al. (2011) achieved success with this approach, which yielded significantly higher count strengths. Such a protocol is illustrated in Fig. 2g (data not yet processed). Over glaciers, GMON requires such an enriched gamma emission setup. The size of the area that is effectively monitored by the GMON ("footprint") extends to 10 m from the detector when there is no snow or water on the ground (Ducharme et al., 2015). The size

of the sensed area exponentially decreases with increasing SWE and is estimated to be of the order of 5 m radius (50 – 100 m²) for 150-300 mm w.e. (Martin et al., 2008; Ducharme et al., 2015). This relatively large foot print is an advantage of this sensor.

With FMCW-Radar technique, as previously stated, penetration depth strongly depends on the measurement frequency. Generally, high frequency instruments result in higher resolution measurements, but these are also affected by greater signal attenuation, i.e., by a reduced depth of penetration. A disadvantage of this approach is that it requires the measurement of snow height as close as possible to the radar sensor. Also, the algorithm for thresholding the radar echo peaks must be developed as well as the calculation of the SWE (see Pomerleau et al., 2020).

GNSS electromagnetic waves can be attenuated under the forest canopy, as the forest transmittivity at 1.5 GHz is not negligible (Wigneron et al., 2017). Yet, because we normalized the signal beneath the snow against the one acquired above the snowpack, when both antennas were placed under the canopy, this effect should not alter retrieval. GNSSr is not well suited to very steep mountainous terrain (e.g., deep-valley bottoms), given that a rather wide sky-view factor is needed by the instrument, and that this view can be limited in such environments, depending on slope and location (Koch et al., 2019, Steiner et al., 2018).

The main conclusions that emerge from Table 3 and the aforementioned remarks are the following, recalling that each approach has its own advantages and limitations (by order of presentation rather than by order of merit):

- The CRNP approach is based on measurements of natural cosmic ray fluxes, which are variable in time, unfortunately requires complementary atmospheric measurements (temperature, pressure and atmospheric humidity) at each site for correcting the signal and must be normalized against a nearby reference site (available worldwide). CRNP on the ground: This is the most efficient system for very deep snowpack (> 2000 mm w.e., perhaps up to 7000 mm w.e.), as is the case in mountain environments or northerly areas that are witness to winter lake-effect snowfall. The most advantageous aspect of the CRNP is its ability to measure SWE through complex snow layers from shallow to deep snow conditions. This is a robust and mature approach, as demonstrated by the French EDF experience (Gottardi et al., 2013; Lejeune et al., 2019); however, the EDF's sensor is based on a system that is not exploited commercially. The alternative sensors are the CRNP-based sensor that is manufactured by Hydroinnova (SnowFox or CRS-1000/B, Hydroinnova, Albuquerque, NM) (<https://hydroinnova.com>) and the CRD manufactured by Alpine Hydromet (www.alpinehydromet.com) and marketed by Geonor Inc. These sensors are relatively new and still need to demonstrate their robustness. The cost of Hydroinnova system is about 11 000 US\$ for sensor only. As previously mentioned, ancillary sensors (atmospheric humidity and barometric pressure sensors) must be added, and the actual price could be up to 17 000 US\$ for full setup. The cost of the Geonor Inc. system is 15 000 US\$.

- CRNP above the snow: The most interesting system for measuring SWE over a large footprint, but it is limited to shallow snowpacks. It is the only approach that can provide an integrated spatial measurement. This approach also needs appropriate adjustment for each site in terms of soil moisture corrections, which can be difficult over a large area.
- GMON: This is one of the most mature instruments for snowpacks that are not too deep (600 mm w.e. according to manufacturer specifications, but up to 800 mm w.e. based on our experience), with a medium footprint (10 m). Yet, it needs systematic site adjustment for soil moisture-induced error, which can increase the bias of measurements, particularly at the end of the winter when the soil becomes potentially saturated during snowmelt. It is the most expensive of the four instruments (around 16 600 US\$, 20 000 \$CAD). This system has proved its robustness and accuracy within the operational Hydro-Quebec Canadian network over a wide variety of environments for almost 10 years (Choquette et al., 2013).
- FMCW-Radar: This approach requires the measurement of the snow depth to be able to retrieve SWE. Its weak point is its limitation in measuring the SWE of wet snow. Yet, the instrument is very useful for dry snowpack characterization, in terms of stratigraphy or for avalanche studies, and also for detection of snowmelt events. Moreover, it is not expensive (1 000 US\$, 800 €). As it is very light weight and compact, one of its strengths is its potential capability to retrieve SWE from remotely piloted aircraft above arctic snowpacks.
- GNSSr: The potential of the GNSSr approach, which is a light and compact system, is strong, given its capability of measuring SWE and LWC with high accuracy, and to derive snow depth. For SWE retrieval, its performance remains very good (relative RMSD of ~10% in the range of 0-1000 mm) and has the capacity to measure deep snowpack (up to 1 500 mm w.e.). SWE accuracy for wet snow has yet to be improved, as it depends upon the GNSS signal processing. Its cost is 8 550 US\$ (7 000 Euros). The station includes the software/license and processing is performed onboard of the station. The Station comes with 1 year of Iridium communication for retrieved product SWE/LWC (via VISTA). VISTA supports customer to find operational way to retrieve data in operational use for future. The license alone for processing the raw data can also be directly purchased at ANavS (<https://anavs.com/>) for 2 370 US\$ (2 000 €).

5. Conclusions

In this paper, we evaluated four types of non-invasive sensors that have all reached a certain level of maturity enabling deployments of autonomous networks for monitoring water equivalent of snow cover (SWE). These include the Cosmic Ray Neutron probe (CRNP), the Gamma Ray Monitoring (GMON) sensor, the frequency-modulated continuous-wave radar at 24 GHz (FMCW-Radar), and the Global Navigation Satellite System receiver (GNSSr) (see Table 1). This new generation of light and practical systems that are based on radiation-wave measurement is now commercially available. The

GMON is already operationally used in Québec, Canada, for hydrological purposes (Hydro-Québec, Rio-Tinto, and governments).

The analysis of their performances that are summarized in Tables 2 (uncertainties of measurement) and 3 (pros and cons) show that each approach has its strengths and weaknesses. The synthesis of their advantages/disadvantages shows that the overall uncertainties remain in the range of manual measurements, i.e., 9 to 15%. CRNP that is placed in the ground beneath the snow is the only system capable of measuring very deep snowpacks, while the GNSSr sensor is limited to SWE up to ~1500 mm w.e., and the two others up to ~800 mm w.e.. Both CRNP and GMON approaches need systematic site adjustments for soil moisture characterization. In addition to SWE, an advantage of the sensor to be considered is their ability to measure other parameters, such as snowpack stratigraphy for the FMCW-Radar, and the liquid water content for the GNSSr. The GNSSr approach, which has relatively low cost and is light and very compact, appears to have a great potential in remote and difficult to access areas.

The requirement of automatic instrumentation networks for SWE measurements to improve seasonal snowpack monitoring is important for several applications, such as where spatially distributed SWE instruments are needed in remote and mountainous areas, for operational water resource and flood management over snow-driven watersheds. Networks of continuous SWE measurements are also required for calibrating satellite-derived SWE information, or for winter transportation safety. This review of continuous-monitoring SWE sensors is intended to help researchers and decision makers choose the one system that is best suited to their needs.

Acknowledgements

We acknowledge all of the students who have contributed to the field measurements, including Amandine Pierre, Maxime Beaudoin-Galaise and Benjamin Bouchard from Université Laval, and Patrick Pomerleau, Fannie Larue and Alex Mavrovic from Université de Sherbrooke. We thank for their support, the staff from Forêt Montmorency and from the Université de Sherbrooke: Patrick Cliche, Patrick Ménard and Gabriel Diab. We also thank Alexandre Vidal, Hydro-Québec, and Vincent Fortin, Environment and Climate Change (ECCC). Finally, the reviewers, together with the following individuals, are thanked for their helpful comments, which improved the article: Craig Smith, ECCC; Charles Fierz, SLF, Davos; Yves Choquette, formerly of IREQ-Hydro-Québec; Florian Appel, VISTA; and Reinhard Kulke, IMST. W.F.J.Parsons English language revision.

Funding:

This project was funded by the Natural Sciences and Engineering Research Council of Canada (NSERC), the Canadian Foundation for Innovation (CFI), Environment and Climate Change Canada (ECCC), and Fonds de recherche du Québec – Nature et technologies (FQRNT), Government of Quebec. The European Space Agency (ESA) contributes to the

896 installation of the GNSSr sensor within the ESA business development demonstration
897 project SnowSense (<https://business.esa.int/projects/snowsense-dp>).
898

899 **Conflicts of interest:**

900 The authors declare absolutely no conflicts of interest or business relationships with any
901 of the manufacturers that are mentioned in this article. The mention of commercial
902 companies or products does not constitute a commercial endorsement of any instrument
903 or manufacturer by the authors.
904
905

Table 2 Uncertainty analysis for the 4 systems that were considered. The Range measurement indicates the highest SWE (mm) value on which the analysis was performed. RMSD: Root Mean Square Difference. R^2 is the determination coefficient of the linear regression analysis. Pts: number of in situ manual samples. “-” means no information available.

Sensor	Reference data	SWE _{max} (mm)	Uncertainty RMSD (mm) (relative RMSD), R^2 (slope, intercept)	References, sites, number of points
CRNP in the ground	Manual snowpit	200	14 mm, $R^2 = 0.96$ (0.78, 8.5 mm)	This study (Fig. 3), 7 pts
	GMON	200	28 mm, $R^2 = 0.89$ (0.79, -3.9 mm)	This study (Fig. 3), 2008-2009 season
	Manual snowpit	1700	–, $R^2 = 0.98$ (0.99, 2.8 mm)	Gottardi et al. (2013) EDF system, Alps and Pyrénées 320 year.sites, 1037 pts.
	Snow core	2500	– (2% ± 13%), $R^2 = 0.943$ (–,–)	Gugerly et al. (2019), Glacier de la Plaine Morte, Switzerland, 9 pts (2 winters)
	–	–	5 – 10%	Hydroinnova snowFox ¹
CRNP above snow	–	–	5 – 10%	Hydroinnova CRS-1000/B ²
GMON	Manual snowpit	500	34 mm (12%), $R^2 = 0.93$ (0.997, 17.1 mm)	This study (Fig. 3 and 4) and Pomerleau et al. (2020), SIRENE et NEIGE-FM, 64 pts
	Snow core	200	40 mm, $R^2 = 0.92$ (1.16, 16.8 mm)	Smith et al., 2017, Sodankylä, Finland, 30 pts
	Snow core	125	23 mm, $R^2 = 0.90$ (0.904, 27.5 mm)	Smith et al., 2017, Caribou Creek, Canada, 19 pts
	Snow core	700	48 mm, $R^2 = 0.92$ (0.881, 32.4 mm)	Smith et al., 2017, Fortress Mountain, Canada, 8 pts
	–	0-300	±15 mm	Campbell Scientific CS725 manual ³
		300-600	±15%	
FMCW-Radar 24 GHz	Manual snowpit	500	38 mm (14%), $R^2 = 0.73$ (0.80, 65.0 mm)	This study (Fig. 4) and Pomerleau et al., 2020, 46 pts, dry snow
	Manual snowpit	750	59 mm (30%), $R^2 = 0.87$ (0.98, 0)	Pomerleau et al., 2020, manual measurements, multi sites Northern Québec, Canada, 78 points dry snow
GNSSr	Manual snowpit	500	32 mm (11%), $R^2=0.93$ (1.05, -7.9 mm)	This study (Fig. 4), 18 points
	Manual snowpit	2000	± 15 mm	SnowSense Vista Inc. manual ⁴ , good conditions
	Manual snowpit	700	23 mm, $R^2 = 0.995$ (0.98, 5.52 mm)	Henkel et al. 2018, Weissfluhjoch, Switzerland (CH)
	Snow-pillow	700	11 mm, $R^2 = 0.999$ (1.01, 1.97 mm)	
	Combined data	800	66 mm, $R^2 = 0.99$ (1.1, -26 mm)	Steiner et al., 2018, Weissfluhjoch, CH, 633 pts
	Manual snowpit	1000	45 mm, $R^2 = 0.98$ (0.98, 31.4 mm) 103 mm, $R^2 = 0.86$ (0.88, 67.3 mm)	Koch et al., 2019 dry snow, Weissfluhjoch, 3 winters Koch et al., 2019 wet snow, Weissfluhjoch, 3 winters
	Snow-pillow and snow scale	1000	30 mm, $R^2 = 0.99$ (0.97, 30.5 mm) 72 mm, $R^2 = 0.93$ (0.92, 65.0 mm)	Koch et al., 2019 dry snow, Weissfluhjoch Koch et al., 2019 wet snow, Weissfluhjoch

1 https://hydroinnova.com/_downloads/snowfox_v1.pdf, Hydroinnova, Albuquerque, NM

2 Hydroinnova, Albuquerque, NM; http://hydroinnova.com/snow_water.html

3 Campbell Scientific (Canada) Corporation, CS725 manual, https://s.campbellsci.com/documents/ca/manuals/cs725_man.pdf.

4 <https://www.vista-geo.de/en/snowsense/>

Table 3 Pro and Cons of the four systems that were considered for SWE monitoring. SM: Soil Moisture. FOV: Field-of-View. The approximate price is given (2021), subject to change according to exchange rate fluctuations.

Sensors	CRNP		GMON	FMCW-Radar 24 GHz	GNSSr
	CRNP on the ground	CRNP above the snow			
SWEmax	Up to 2000 mm	~150-300 mm	600 mm (possibly 800 mm)	~1000 mm	Up to 1500 mm
Other measured parameters	-	SM	SM	Melt detection	LWC, SD (estimated)
Other sensors needed	P, T _{air} , RH	P, T _{air} , RH	–	SD	–
Typical sampling rate	Discontinuous ^a	Discontinuous ^a	Discontinuous ^a	Continuous	Not strictly continuous ^b
Footprint	~1 - 2 m ²	20-40 ha (300 000 m ²)	FOV 60° Typically, 50-100 m ² *	FOV ±32.5° azimuth and ±12° elevation, 0.4 m ² *	~1 m ²
Price (US\$, 2021)	Hydroinnova: 11 000 (sensor only) EDF: Not marketed (on request) ^c		16 600 (sensor only)	1 000 (radar and software ^d)	8 550 (complete station ^e)
Power consumption	0.02 W, 12 V DC		0.18 W, 12 V DC	Operating: 8.14 W, 15 V DC	Operating 5 W, 12 V DC
Main advantage	Very deep snowpack	Large footprint	Medium footprint	Snowpack microstructure Very light and compact Low cost	Light SD and LWC Low cost (license only)
Main inconvenience	SM issue Needs ancillary measurements	SM knowledge needed, Needs ancillary measures Shallow snowpack	SM knowledge needed	Dry snow only	Large sky view factor required
Other drawbacks	EDF system not commercially available	Need further validation	Cost	Not turnkey Issue with ice crust	SWE for wet snow must be improved Retrieval algo. issue
Main applications, Capability (see text) Comments	Hydrology Network operational by EDF ^c	Hydrology, SM	Hydrology, SM Network operational by Hydro-Québec	SM, Stratigraphy, Avalanche, Melting monitoring Lake ice thickness RPA capability ^f	Hydrology, SM Avalanche, Melt monitoring

a: Counts must be accumulated over a specified period, e.g. 6h, 12h, or longer. b: GNSS signals must be averaged over a period of time for noise reduction; the typical measurement cycle: 1 per day (possibly up to 6 per day). c: System based on a sensor that is not commercialized. d: Software for sensor settings and reading/recording data, but not for SWE retrievals. e: Subscription license required. f: Remotely Piloted Aircraft capability.

* Depending on the height of the sensor on its support mast above snow, Field-of-View (FOV) given for 3 m mast.

Appendix or Supplementary data

Estimating the uncertainty of in-situ field measurements

In situ field measurements of Snow Water Equivalent (SWE) are accompanied by uncertainties from a variety of sources, which include: 1) instrumental: size and type of sampling tube according to snow depth, weight scale; 2) sampling technique, extracting the snow core; 3) error that is induced by observer; 4) snow conditions: local natural variability, ice lenses and hard snow crusts within the snowpack; 5) soil conditions: irregular soil surface, identification of snow-ground interface. Snow depth is sometimes difficult to estimate over a thawed organic snow-ground interface because surface organic material is often taken into account in the snowpack depth estimate using a snow height probe.

In general, the uncertainty in the SWE depends mainly upon the diameter of the snow core according to the snow depth (the deeper the snow, the smaller the snow core that is required). Few studies discuss the accuracy of in-situ SWE measurements comprehensively over a large range of conditions, from 100 to more than 2 000 mm w.e. For example, the standard protocol that is implemented by Environment and Climate Change Canada is to attain five to ten measurements along a pre-determined survey line of about 150 to 300 m using a translucent plastic ESC-30 sampler (6.2 cm Ø, which is commonly employed in Canada) (Brown et al., 2019). Each study is generally focused on one type of snowpack. Commonly, relative uncertainty varies from 6% for shallow snowpack (0-300 mm w.e.) to 8% (300 – 1000 mm w.e.) for medium snowpack to 10-12 % for deeper snowpack (> 1000 mm w.e.) (see references in the recent review by López-Moreno et al., 2020; also see Work et al., 1965; Turcan and Loijens, 1975; Peterson and Brown, 1975; Goodison et al., 1981 and 1987; Sturm et al., 2010; Berezovskaya and Kane, 2007; Dixon and Boon, 2012; Stuefer et al., 2013; Steiner et al., 2018; Gugerli et al., 2019; Brown et al., 2019). Among recent studies, Stuefer et al. (2013) and López-Moreno et al. (2020) are limited to shallow Arctic snowpack, Steiner et al. (2018) to medium snowpack (up to 1200 mm w.e.), while Gugerli et al. (2019) discuss the problem across a large SWE range of alpine snowpacks over a glacier from 200 to 2300 mm w.e., but with the same snow core (Fig. A1).

In summary, it is well known that SWE uncertainty decreases for shallow snowpack with a larger snow core diameter (typically above 6 cm diameter), given that a larger volume of snow is sampled. Yet, on the other hand, the coring technique is more difficult when snow depth increases. For thicker snowpack, it requires the digging of a pit, because a larger core diameter impeded the retrieval of the snow sample directly from the top of the snow surface. Thus, a large snow corer is limited to shallow snowpacks (snow depth less than 1.5 – 2 m). Moreover, commonly remarks from both our experience and the above cited studies agree in that uncertainties in SWE estimates increase with thicker snowpacks. A small diameter snow core is required for thick snowpacks (snow depth above 2 m).

Figure A2 illustrates the underestimation of SWE with a large diameter snow corer when SWE increases, from a large dataset that was derived from our International Polar Year experiments (Langlois et al., 2010).

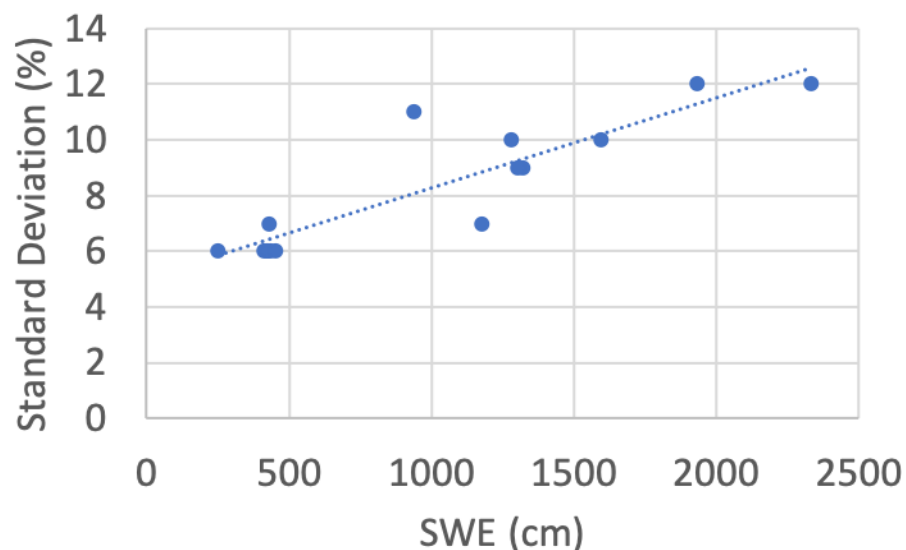


Figure A1 Relationship between the standard deviation (%) of SWE measurements as a function of SWE (mm) based on snow core, derived from Gugerli et al. (2109) (data from Glacier de la Plaine Morte, Switzerland,). Results show an uncertainty of 6 % for SWE of the order of 250 – 500 mm, about 10% for SWE between 1000 and 1500 mm, and 12% for SWE between 2000 – 2500 mm.

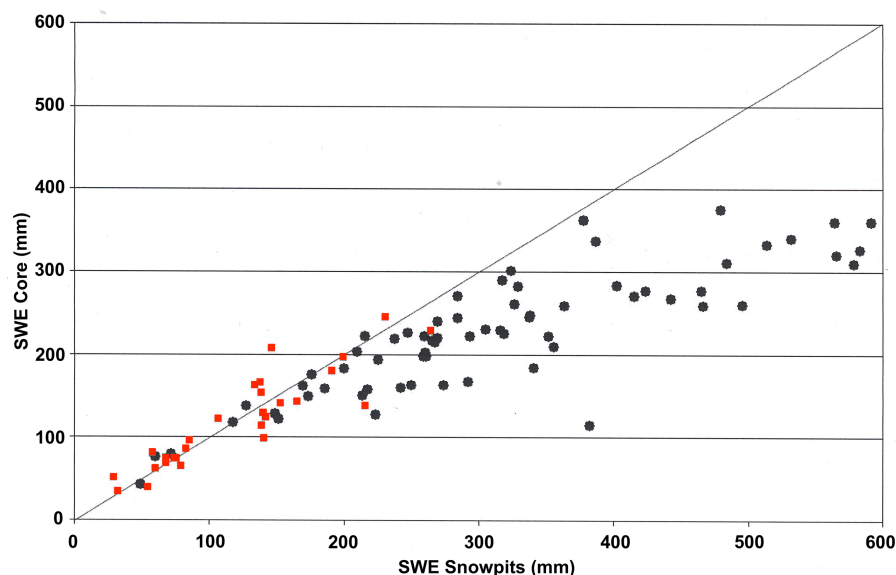


Figure A2. Comparison between SWE measurements (in mm) from snow core and snowpit methods. Red squares are for small diameter snow core (ESC-30 type core: 6.2 cm) and black points are for large diameter snow cores (9.5 cm). The black line is $Y=X$. Measured SWE Core values are clearly underestimated above 250-300 mm SWE. Unfortunately, no measurements with small diameter snow cores above 280 mm SWE are present in this example. The database (94 points) is derived from the International Polar Year project (Langlois et al., 2010), including sampling sites at Sherbrooke (SIRENE, 45.37° N; -71.92° W), Sept-Iles (50.30° N; -66.28° W), Schefferville (54.90° N; -66.70° W) and Kuujuaq (58.06° N; -71.95° W) (also see Royer et al., 2021).

References

For references related to a sensor, the name of the sensor has been highlighted in **bold**.

- Alonso, R., Pozo, J.M.G.d., Buisán, S.T., and Álvarez, J.A.: Analysis of the Snow Water Equivalent at the AEMet-Formigal Field Laboratory (Spanish Pyrenees) during the 2019/2020 winter season using a Stepped-Frequency Continuous Wave Radar (SFCW), *Remote Sens.*, 13, 616. <https://doi.org/10.3390/rs13040616>, 2021. (**SFCW radar**)
- Andreasen, M., Jensen, K. H., Desilets, D., Franz, T., Zreda, M., Bogen, H., and Looms, M.C.: Status and perspectives of the cosmic-ray neutron method for soil moisture estimation and other environmental science applications. *Vadose Zone J.*, 16, 1–11. doi: 10.2136/vzj2017.04.0086, 2017. (**CRNP**)
- Appel, F., Koch, F., Rösel, A., Klug, P., Henkel, P., Lamm, M., Mauser, W., and Bach, H.: Advances in Snow Hydrology Using a Combined Approach of GNSS In Situ Stations, Hydrological Modelling and Earth Observation—A Case Study in Canada. *Geosciences*, 9, 44. <https://doi.org/10.3390/geosciences9010044>, 2019. (**GNSSr**)
- Berezovskaya, S. and Kane, D. L.: Strategies for measuring snow water equivalent for hydrological applications: Part 1, accuracy of measurements. *Proceedings of 16th Northern Research Basin Symposium, Petrozavodsk, Russia*, 22–35, 2007. (**Snow core**)
- Bissell, V.C., and Peck, E.L.: Monitoring snow water equivalent by using natural soil radioactivity. *Water Resour. Res.*, 9, 885–890, 1973. (**GMON**)
- Bogen, H.R., Herrmann, F., Jakobi, J., Brogi, C., Ilias, A., Huisman, J.A., Panagopoulos, A., and Pissinaras, V.: Monitoring of Snowpack Dynamics with Cosmic-Ray Neutron Probes: A Comparison of Four Conversion Methods. *Front. Water*, 2, 19, doi: 10.3389/frwa.2020.00019, 2020. (**CRNP**)
- Bormann, K.J., Westra, S., Evans, J.P., and McCabe, M.F.: Spatial and temporal variability in seasonal snow density. *J. Hydrol.*, 484, 63–73, 2013. (**Snow core**)
- Brown, R.D., Fang, B., and Mudryk, L.: Update of Canadian Historical Snow Survey Data and Analysis of Snow Water Equivalent Trends, 1967–2016, *Atmosphere-Ocean*, DOI: 10.1080/07055900.2019.1598843, 2019. (**Snow core**)
- Brown, R.D., Smith, C., Derksen, C., and Mudryk, L.: Canadian In Situ Snow Cover Trends for 1955–2017 Including an Assessment of the Impact of Automation, *Atmosphere-Ocean*, DOI: 10.1080/07055900.2021.1911781, 2021.
- Carroll, T. R.: Airborne Gamma Radiation Snow Survey Program: A user's guide, Version 5.0. National Operational Hydrologic Remote Sensing Center (NOHRSC), Chanhassen, 14, <https://www.nohrsc.noaa.gov/snowsurvey/>, 2001. (**GMON**)
- Choquette, Y., Ducharme, P., and Rogoza, J.: CS725, an accurate sensor for the snow water equivalent and soil moisture measurements, in: *Proceedings of the International Snow Science Workshop, Grenoble, France, 7–11 October 2013*, 2013 (**GMON**)
- Clark, M. P., Hendrikx, J., Slater, A. G., Kavetski, D., Anderson, B., Cullen, N. J., Kerr, T., Hreinsson, E. Ö., and Woods, R. A.: Representing spatial variability of snow water equivalent in hydrologic and land-surface models: A review, *Water Resour. Res.*, 47, W07539, doi:10.1029/2011WR010745, 2011.
- Delunel, R., Bourles, D. L., van der Beek, P. A., Schlunegger, F., Leya, I., Masarik, J. and Paquet, E.: Snow shielding factors for cosmogenic nuclide dating inferred from long-term neutron detector monitoring, *Quat. Geochronol.*, 24, 16–26, doi:10.1016/j.quageo.2014.07.003, 2014. (**CRNP**)
- Desilets, D., and Zreda, M.: Footprint diameter for a cosmic-ray soil moisture probe: Theory and Monte Carlo simulations, *Water Resour. Res.*, 49, 3566–3575, 2013. (**CRNP**)
- Desilets, D., Zreda, M., and Ferré, T.P.A.: Nature's neutron probe: Land surface hydrology at an elusive scale with cosmic rays, *Water Resour. Res.*, 46, 1–7, 2010. (**CRNP**)
- Desilets, D.: Calibrating a non-invasive cosmic ray soil moisture probe for snow water equivalent, *Hydroinnova Technical Document 17-01*, doi:10.5281/zenodo.439105, 2017. (**CRNP**)
- Dixon, D., and Boon, S.: Comparison of the SnowHydro snow sampler with existing snow tube designs. *Hydrologic Processes*, 20, 2555–2562, DOI: 10.1002/hyp.9317, 2012. (**Snow core**)
- Dong, C.: Remote sensing, hydrological modeling and in situ observations in snow cover research: A review. *J. Hydrol.*, 561 (2018) 573–583, 2018.
- Ducharme, P., Houdayer, A., Choquette, Y., Kapfer, B., and Martin, J. P.: Numerical Simulation of Terrestrial Radiation over A Snow Cover. *J. Atmos. Ocean. Technol.*, 32, 1478–1485, 2015. (**GMON**)
- Ellerbruch, D., and Boyne, H.: Snow Stratigraphy and Water Equivalence Measured with an Active Microwave System. *J. Glaciol.* 26, 225–233, 1980. (**FMCW-Radar**)

- Evans, J. G., Ward, H. C., Blake, J. R., Hewitt, E. J., Morrison, R., Fry, M., Ball, L. A., Doughty, L. C., Libre, J. W., Hitt, O. E., Rylett, D., Ellis, R. J., Warwick, A. C., Brooks, M., Parkes, M. A., Wright, G. M. H., Singer, A. C., Boorman, D. B., and Jenkins, A.: Soil water content in southern England derived from a cosmic-ray soil moisture observing system - COSMOS-UK. *Hydrological Processes*, 30(26), 4987–4999. <https://doi.org/10.1002/hyp.10929>, 2016.
- Fujino, K., Wakahama, G., Suzuki, M., Matsumoto, T., and Kuroiwa, D.: Snow stratigraphy measured by an active microwave sensor. *Ann. Glaciol.*, 6, 207–210, 1985. **(FMCW-Radar)**
- GCOS-WMO: The global observing system for climate: implementation needs, World Meteorological Organization, Geneva, Switzerland, 2016. <https://public.wmo.int/en/programmes/global-climate-observing-system>
- Goodison, B., Ferguson, H., and McKay, G.: Measurement and data analysis, in handbook of snow: principles, processes, management, and use, Pergamon press Canada, Toronto, Canada, 191-274, 1981. **(Snow core)**
- Goodison, B.E., Glynn, J.E., Harvey, K.D., and Slater, J.E.: Snow Surveying in Canada: A Perspective, *Can. Water Resour. J.*, 12:2, 27-42, DOI: 10.4296/cwrj1202027, 1987. **(Snow core)**
- Gottardi, F., Carrier, P., Paquet, E., Laval, M.-T., Gailhard, J., and Garçon, R.: Le NRC: Une décennie de mesures de l'équivalent en eau du manteau neigeux dans les massifs montagneux français. In *Proceedings of the International Snow Science Workshop Grenoble*, 7–11 October 2013, 926–930, 2013. **(CRNP)**
- Gray, D. M., Granger, R. J., and Dyck, G. E.: Over winter soil moisture changes, *Transactions of ASAE*, 28, 442–447, 1985.
- Gray, D. M., Toth, B., Zhao, L., Pomeroy, J. W., and Granger, R. J.: Estimating areal snowmelt infiltration into frozen soils, *Hydrol. Process.*, 15, 3095–3111, 2001.
- GPRI brochure: GAMMA Portable Radar Interferometer (GPRI) https://gamma-rs.ch/uploads/media/Instruments_Info/gpri2_brochure_20160708.pdf, 2021. **(Radar)**
- Gugerli, R., Salzmann, N., Huss, M., and Desilets, D.: Continuous and autonomous snow water equivalent measurements by a cosmic ray sensor on an alpine glacier, *The Cryosphere*, 13, 3413–3434, <https://doi.org/10.5194/tc-13-3413-2019>, 2019. **(CRNP and Snow core)**
- Gunn, G.E., Duguay, C.R., Brown, L.C., King, J., Atwood, D., and Kasurak, A.: Freshwater Lake Ice Thickness Derived Using Surface-based X- and Ku-band FMCW Scatterometers. *Cold Reg. Sci. Technol.*, 120, 115–126, 2015. **(FMCW-Radar)**
- Henkel, P., Koch, F., Appel, F., Bach, H., Prasch, M., Schmid, L., Schweizer, J., and Mauser, W.: Snow water equivalent of dry snow derived from GNSS Carrier Phases. *IEEE Trans. Geosci. Remote Sens.*, 56(6), 3561–3572. <https://doi.org/10.1109/TGRS.2018.2802494>, 2018. **(GNSSr)**
- Hu, X., Ma, C., Hu, R., and Yeo, T. S.: Imaging for Small UAV-Borne FMCW SAR. *Sensors*, 19, 87, doi: 10.3390/s19010087, 2019. **(FMCW-Radar)**
- IMST: IMST sentireTM Radar Module 24 GHz sR-1200 Series User Manual. Available online: <http://www.radar-sensor.com/>, 2021 **(FMCW-Radar)**
- Jitnikovitch, A., Marsh, P., Walker, B., and Desilets, D.: Cosmic-ray neutron method for the continuous measurement of Arctic snow accumulation and melt, *The Cryosphere Discuss.* [preprint], <https://doi.org/10.5194/tc-2021-124>, in review, 2021. **(CRNP)**
- Key, J., Goodison, B., Schöner, W., Godøy, Ø., Ondráš, M., and Snorrason, Á.: A Global Cryosphere Watch. *Arctic*, 68, 1, 48 – 58. <http://dx.doi.org/10.14430/arctic4476>, 2015.
- Key, J., Schöner, W., Fierz, C., Citterio, M., and Ondráš, M.: Global Cryosphere Watch (GCW) implementation plan, World Meteorological Organization, Geneva, Switzerland, https://globalcryospherewatch.org/reference/documents/files/GCW_IP_v1.7.pdf, 2016.
- Kinar, N. J., and Pomeroy, J. W.: Measurement of the physical properties of the snowpack. *Rev. Geophys.* 53, 481–544. doi: 10.1002/2015RG000481, 2015.
- King J., Kelly, R., Kasurak, A., Duguay, C., Gunn, G., Rutter, N., Watts, T., and Derksen C.: Spatio-temporal influence of tundra snow properties on Ku-band (17.2 GHz) backscatter. *J. Glaciol.*, 61(226), doi: 10.3189/2015JoG14J020, 2015. **(Radar)**
- Kirkham, J.D., Koch, I., Saloranta, T.M., Litt, M., Stigter, E.E., Møen, K., Thapa, A., Melvold, K., and Immerzeel, W.W.: Near Real-Time Measurement of Snow Water Equivalent in the Nepal Himalayas. *Front. Earth Sci.* 7:177. doi: 10.3389/feart.2019.00177, 2019. **(GMON)**
- Koch, F., Henkel, P., Appel, F., Schmid, L., Bach, H., Lamm, M., Prasch, M., Jürg Schweizer, J., and Mauser, W.: Retrieval of snow water equivalent, liquid water content, and snow height of dry and wet snow by combining GPS signal attenuation and time delay. *Water Resour. Res.*, 55, 4465–4487. <https://doi.org/10.1029/2018WR024431>, 2019. **(GNSSr)**

- Koh, G., Yankielun, N.E., and Baptista, A.I.: Snow cover characterization using multiband FMCW radars. *Hydrol. Process.*, 10, 1609–1617, 1996. **(FMCW-Radar)**
- Kramer, D., Langlois, A., Royer, A., Madore, J.-B., King, J., McLennan, D. and Boisvert-Vigneault, É.: Assessment of Arctic snow stratigraphy and water equivalent using a portable Frequency Modulated Continuous Wave RADAR. Submitted to *Cold Regions Science and Technology*, ID.: CRST-D-21-00297, (2021).
- Laliberté, J., Langlois, A., Royer, A., Madore, J.-B., and Gauthier, F.: Retrieving high contrasted interfaces in dry snow using a frequency modulated continuous wave (FMCW) Ka-band radar: a context for dry snow stability, *Physical Geography*, In revision (TPHY-S-21-00044), 2021. **(FMCW-Radar)** **To be updated**
- Langlois, A., Royer, A. and Goïta, K.: Analysis of simulated and spaceborne passive microwave brightness temperature using in situ measurements of snow and vegetation properties. *Can J Remote Sens.* 36(S1), 135–148. doi:10.5589/m10-016, 2010.
- Langlois, A.: Applications of the PR Series Radiometers for Cryospheric and Soil Moisture Research. Publisher: Radiometrics Corporation
[https://www.researchgate.net/publication/299372180 Applications of the PR Series Radiometers for Cryospheric and Soil Moisture Research](https://www.researchgate.net/publication/299372180_Applications_of_the_PR_Series_Radiometers_for_Cryospheric_and_Soil_Moisture_Research), 2015. **(Radiometer)**
- Larson, K. M., and Small, E. E.: Normalized microwave reflection index: A vegetation measurement derived from GPS networks, *IEEE J. Sel. Topics Appl. Earth Observ. Remote Sens.*, 7(5), 1501-1511, doi: 10.1109/JSTARS.2014.2300116, 2014. **(GNSSr)**
- Larson, K. M.: GPS interferometric reflectometry: Applications to surface soil moisture, snow depth, and vegetation water content in the western United States. *Wiley Interdisciplinary Reviews: Water*, 3(6), 775–787. <https://doi.org/10.1002/wat2.1167>, 2016. **(GNSSr)**
- Larson, K., Gutmann, E., Zavorotny, V., Braun, J., Williams, M., and Nievinski, F.: Can we measure snow depth with GPS receivers? *Geophys. Res. Lett.*, 36, L17502. <https://doi.org/10.1029/2009GL039430>, 2009. **(GNSSr)**
- Larue, F., Royer, A., De Sève, D., Roy, A., Picard, G., Vionnet, V.: Simulation and assimilation of passive microwave data using a snowpack model coupled to a calibrated radiative transfer model over North-Eastern Canada, *Water Resour. Res.*, 54, 4823–4848, <https://doi.org/10.1029/2017WR022132>, 2018.
- Leinss, S., Wiesmann, A., Lemmetyinen, J., and Hajnsek, I.: Snow Water Equivalent of Dry Snow Measured by Differential Interferometry. *IEEE J. Sel. Topics Appl. Earth Observ. Remote Sens.*, 8(8), 3773-379, 2015. **(SnowScat radar)**
- Lejeune, Y., Dumont, M., Panel, J.-M., Lafaysse, M., Lapalus, P., Le Gac, E., Lesaffre, B., and Morin, S.: 57 years (1960–2017) of snow and meteorological observations from a mid-altitude mountain site (Col de Porte, France, 1325 m of altitude), *Earth Syst. Sci. Data*, 11, 71–88, <https://doi.org/10.5194/essd-11-71-2019>, 2019.
- López-Moreno, J.I., Leppänen, L., Luks, B., Holko, L., Picard, G., Sanmiguel-Valladolid, A., Alonso-González, E., Finger, D.C., Arslan, A.N., Gillemot, K., Sensoy, A., Sorman, A., Ertaş, M. C., Fassnacht, S.R., Fierz, C., and Marty, C.: Intercomparison of measurements of bulk snow density and water equivalent of snow cover with snow core samplers: Instrumental bias and variability induced by observers. *Hydrol. Proc.*, 34, 3120–3133, <https://doi.org/10.1002/hyp.13785>, 2020. **(Snow core)**
- Marshall, H.-P., and Koh, G.: FMCW radars for snow research. *Cold Reg. Sci. Technol.*, 52, 118–131, 2008.
- Marshall, H.-P., Schneebeli, M., and Koh, G. Snow stratigraphy measurements with high-frequency FMCW radar: Comparison with snow micro-penetrometer. *Cold Reg. Sci. Technol.*, 47, 108–117, 2007. **(FMCW-Radar)**
- Marshall, H.-P., Koh, G., and Forster, R.: Estimating alpine snowpack properties using FMCW radar. *Ann. Glaciol.*, 40, 157–162, 2005. **(FMCW-Radar)**
- Martin, J.-P., Houdayer, A., Lebel, C., Choquette, Y., Lavigne, P., and Ducharme, P.: An unattended gamma monitor for the determination of snow water equivalent (SWE) using the natural ground gamma radiation. 2008 IEEE Nuclear Science Symposium and Medical Conference, P. Sellin, Ed., IEEE, 983–988, 2008. **(CRNP)**
- Matzler, C.: Microwave permittivity of dry snow, *IEEE Trans. Geosci. Remote Sens.*, 34, 573–581, <https://doi.org/10.1109/36.485133>, 1996.
- Meloche, J., Langlois, A., Rutter, N., Royer, A., King, J., and Walker, B.: Characterizing Tundra snow sub-pixel variability to improve brightness temperature estimation in satellite SWE retrievals, *The Cryosphere Discussion* (Submitted to-2021-156), 2021. **To be updated**
- Meredith, M., Sommerkorn, M., Cassotta, S., Derksen, C., Ekaykin, A., Hollowed, A., Kofinas, G., Mackintosh, A., Melbourne-Thomas, J., Muelbert, M.M.C., Ottersen, G., Pritchard, H., Schuur, E.A.G.: Polar Regions. In: IPCC Special Report on the Ocean and Cryosphere in a Changing Climate [H.-O. Pörtner, D.C. Roberts, V. Masson-Delmotte, P. Zhai,

- M. Tignor, E. Poloczanska, K. Mintenbeck, A. Alegría, M. Nicolai, A. Okem, J. Petzold, B. Rama, N.M. Weyer (eds.)). <https://www.ipcc.ch/srocc/chapter/chapter-3-2/>, 2019.
- Murray, R. M., and Holbert, K. E.: Nuclear Energy: An Introduction to the Concepts, Systems, and Applications of Nuclear Processes, Eighth Edition, Imprint Butterworth-Heinemann, Elsevier Inc., 624 p. <https://doi.org/10.1016/C2016-0-04041-X>, 2020. **(CRNP)**
- Okorn, R., Brunnhofer, G., Platzer, T., Heilig, A., Schmid, L., Mitterer, C., Schweizer, J., and Eisen, O.: Upward-looking L-band FMCW radar for snow cover monitoring. *Cold Reg. Sci. Technol.*, 103, 31–40, 2014. **(FMCW-Radar)**
- Paquet, E. and Laval, M.T.: Retour d'expérience et perspectives d'exploitation des Nivomètres à Rayonnement Cosmique d'EDF / Operation feedback and prospects of EDF Cosmic-Ray Snow Sensors. *La Houille Blanche* 2006-2, 113-119, 2006. **(CRNP)**
- Paquet, E., Laval, M., Basalaev, L. M., Belov, A., Eroshenko, E., Kartyshev, V., Struminsky, A., and Yanke, V.: An application of cosmic-ray neutron measurements to the determination of the snow-water equivalent, *Proc. 30th Int. Cosm. Ray Conf.*, Mexico City, Mexico, 2008, 1, 761– 764, 2008. **(CRNP)**
- Peng, Z., and Li, C.: Portable Microwave Radar Systems for Short-Range Localization and Life Tracking: A Review, *Sensors*, 19, 1136, 2019. **(FMCW-Radar)**
- Peterson, N., and Brown, J.: Accuracy of snow measurements, In *Proceedings of the 43rd Annual Meeting of the Western Snow Conference*, Coronado, California, 1-5, 1975. **(Snow core)**
- Pieraccini, M., and Miccinesi, L.: Ground-Based Radar Interferometry: A Bibliographic Review, *Remote Sens.*, 11(9), 1029, 2019. <https://doi.org/10.3390/rs11091029>. **(Radar)**
- Pirazzini, R., Leppänen, L., Picard, G., López-Moreno, J. I., Marty, C., Macelloni, G., Kontu, A., von Lerber, A., Tanis, C. M., Schneebeli, M., de Rosnay, P., and Arslan, A. N.: European in-situ snow measurements: practices and purposes, *Sensors*, 18, 2016. doi: 10.3390/s18072016, 2018.
- Pomerleau, P., Royer, A., Langlois, A., Cliche, P., Courtemanche, B., Madore, J.B., Picard, G. and Lefebvre, É.: Low Cost and Compact FMCW 24 GHz Radar Applications for Snowpack and Ice Thickness Measurements, *Sensors* 20, 14, 3909. <https://doi.org/10.3390/s20143909>, 2020. **(FMCW-Radar)**
- Prince, M., Roy, A., Royer, A., and Langlois, A.: Timing and Spatial Variability of Fall Soil Freezing in Boreal Forest and its Effect on SMAP L-band Radiometer Measurements, *Remote Sens. Environ.*, 231, 111230, 2019.
- Proksch, M., Rutter, N., Fierz, C., and Schneebeli, M.: Intercomparison of snow density measurements: Bias, precision, and vertical resolution, *Cryosphere*, 10, 371–384, 2016.
- Rasmussen, R., Baker, B., Kochendorfer, J., Meyers, T., Landolt, S., Fischer, A. P., Black, J., Thériault, J. M., Kucera, P., Gochis, D., Smith, C., Nitu, R., Hall, M., Ikeda, K., and Gutmann, E.: How Well Are We Measuring Snow: The NOAA/FAA/NCAR Winter Precipitation Test Bed, *Bull. Am. Meteorol. Soc.*, 93, 811–829, 2012. **(Snow core)**
- Rodriguez-Morales, F., Gogineni, S., Leuschen, C.J., Paden, J.D., Li, J., Lewis, C. C., Panzer, B., Alvestegui, D. G-G., Patel, A., Byers, K., Crowe, R., Player, K., Hale, R., Arnold, E., Smith, L., Gifford, C., Braaten, D., and Panton, C.: Advanced multifrequency radar instrumentation for polar research. *IEEE Trans. Geosci. Remote Sens.* 52, 2824–2842, 2014. **(FMCW-Radar)**
- Roy, A., Royer, A., St-Jean-Rondeau, O., Montpetit, B., Picard, G., Mavrovic, A., Marchand, N., and Langlois, A.: Microwave snow emission modeling uncertainties in boreal and subarctic environments, *The Cryosphere*, 10, 623-638, <http://www.the-cryosphere.net/10/623/2016/> doi:10.5194/tc-10-623-2016, 2016. **(Radiometer)**
- Roy, A., Toose, P., Williamson, M., Rowlandson, T., Derksen, C., Royer, A., Berg, A., Lemmetyinen, J., and Arnold, L.: Response of L-Band brightness temperatures to freeze/thaw and snow dynamics in a prairie environment from ground-based radiometer measurements, *Remote Sens. Environ.*, 191, 67-80, 2017. **(Radiometer)**
- Rutter, N., Sandells, M. J., Derksen, C., King, J., Toose, P., Wake, L., Watts, T., Essery, R., Roy, A., Royer, A., Marsh, P., Larsen, C., and Sturm, M.: Effect of snow microstructure variability on Ku-band radar snow water equivalent retrievals, *The Cryosphere*, 13, 3045–3059, <https://doi.org/10.5194/tc-13-3045-2019>, 2019.
- Rutter, N., Sandells, M., Derksen, C., Toose, P., Royer, A., Montpetit, B., Lemmetyinen, J., and Pulliainen, J.: Snow stratigraphic heterogeneity within ground-based passive microwave radiometer footprints: implications for emission modeling, *J. Geophys. Res. Earth Surf.*, 199, 550–565, <https://doi.org/10.1002/2013JF003017>, 2014.
- Schattan, P., Baroni, G., Oswald, S. E., Schöber, J., Fey, C., Kormann, C., Huttenlau, M., and Achleitner, S.: Continuous monitoring of snowpack dynamics in alpine terrain by aboveground neutron sensing, *Water Resour. Res.*, 53, 3615–3634, doi: 10.1002/2016WR020234, 2017. **(CRNP)**

- Schneider, M.: Automotive radar—Status and trends. In Proceedings of the German Microwave Conference, Ulm, Germany, 5–7 April 2005; pp. 144–147, 2005. **(FMCW-Radar)**
- Shah, R., Xiaolan Xu, Yueh, S., Sik Chae, C., Elder, K., Starr, B., and Kim, Y.: Remote Sensing of Snow Water Equivalent Using P-Band Coherent Reflection, IEEE Geosci. Remote Sens. Lett., 14, 3, 309–313, doi: 10.1109/LGRS.2016.2636664, 2017. **(GNSSr)**
- Sigouin, M. J. P., and Si, B. C.: Calibration of a non-invasive cosmic-ray probe for wide area snow water equivalent measurement. Cryosphere, 10, 1181–1190, 2016 www.the-cryosphere.net/10/1181/2016/, 2016. **(CRNP)**
- Smith, C. D., Kontu, A., Laffin, R., and Pomeroy, J. W.: An assessment of two automated snow water equivalent instruments during the WMO solid precipitation intercomparison experiment, Cryosphere, 11, 101–116. doi: 10.5194/tc-11-101-2017, 2017. **(GMON)**
- Steiner, L., Meindl, M., Fierz, C., and Geiger, A.: An assessment of sub-snow GPS for quantification of snow water equivalent, The Cryosphere, 12, 3161–3175, <https://doi.org/10.5194/tc-12-3161-2018>, 2018. **(GNSSr)**
- Steiner, L., Meindl, M., and Geiger, A.: Characteristics and limitations of GPS L1 observations from submerged antennas, J. Geodesy, 93, 267–280, <https://doi.org/10.1007/s00190-018-1147-x>, 2019. **(GNSSr)**
- Stranden, H. B., Ree, B. L., and Møen, K. M.: Recommendations for Automatic Measurements of Snow Water Equivalent in NVE. Report of the Norwegian Water Resources and Energy Directorate, Majorstua, Oslo, Norway, 34 p., 2015. **(GMON)**
- Stuefer, S., Kane, L. D., and Liston, G. E.: In situ snow water equivalent observations in the US Arctic, Hydrol. Res., 44, 21–34, <https://doi.org/10.2166/nh.2012.177>, 2013. **(Snow core)**
- Sturm, M., Taras, B., Liston, G., Derksen, C., Jones, T., and Lea J.: Estimating snow water equivalent using snow depth data and climate classes. Journal of Hydrometeorology, 11, 1380–1394, 2010. **(Snow core)**
- Tiuri, M., Sihvola, A., Nyfors, E., and Hallikainen, M.: The complex dielectric constant of snow at microwave frequencies. IEEE J. Ocean. Eng., 9, 377–382, 1984.
- Turcan, J., and Loijens, J.: Accuracy of snow survey data and errors in snow sampler measurements, Proc. 32nd East. Snow. Conf., 2-11, 1975. **(Snow core)**
- Vather, T., Everson, C. S., and Franz, T. E.: The applicability of the cosmic ray neutron sensor to simultaneously monitor soil water content and biomass in an Acacia mearnsii Forest. Hydrology, 7(3), 48. <https://doi.org/10.3390/hydrology7030048>, 2020. **(CRNP)**
- Vriend, N.M., McElwaine, J.N., Sovilla, B., Keylock, C.J., Ash, M., and Brennan, P. V.: High-resolution radar measurements of snow avalanches, Geophys. Res. Lett., 40, 727–731, 2013. **(FMCW-Radar)**
- Wallbank, J.R., Cole, S.J., Moore, R.J., Anderson, S.R., Mellor, E.J.: Estimating snow water equivalent using cosmic-ray neutron sensors from the COSMOS-UK network. Hydrological Processes, 35:e14048. <https://doi.org/10.1002/hyp.14048>, 2021. **(CRNP)**
- Werner, C., Suess, M., Wegmüller, U., Frey, O., and Wiesmann A.: The Esa Wideband Microwave Scatterometer (Wbscat): Design and Implementation, in Proc. IGARSS 2019 - IEEE International Geoscience and Remote Sensing Symposium, 8339–8342, doi: 10.1109/IGARSS.2019.8900459, 2019. **(SnowScat)**
- Werner, C., Wiesmann, A., Strozzi, T., Schneebeli, M., and Mätzler, C.: The SnowScat ground-based polarimetric scatterometer: Calibration and initial measurements from Davos Switzerland, in Proc. IEEE Int. Geosci. Remote Sens. Symp. (IGARSS'10), Jul. 2010, 2363–2366, 2010. **(SnowScat)**
- Wiesmann, A., Werner, C., Strozzi, T., Matzler, C., Nagler, T., Rott, H., Schneebeli, M., and Wegmüller, U.: SnowScat, X-to Ku-Band Scatterometer Development, in Proc. of ESA Living Planet Symposium, Bergen 28.6. - 2.7. https://gamma-rs.ch/uploads/media/Instruments_Info/gamma_snowscat.pdf, 2010. **(SnowScat)**
- Wiesmann, A., Werner, C., Wegmüller, U., Schwank, M., and Matzler, C.: ELBARA II, L-band Radiometer for SMOS Cal/Val Purposes, https://gamma-rs.ch/uploads/media/Instruments_Info/ELBARAII_poster.pdf, 2021. **(Radiometer)**
- Wigneron, J.P., Jackson, T.J., O'Neill, P., De Lannoy, G.J., de Rosnay, P., Walker, J.P., Ferrazzoli, P., Mironov, V., Bircher, S., Grant, J.P., Kurum, M., Schwank, M., Munoz-Sabater, J., Das, N., Royer, A., Al-Yaari, A., Bitar, A. Fernandez-Moran, R., Lawrence, H., Mialon, A., Parrens, M., Richaume, P., Delwart, S., and Kerr Y.: Modelling the passive microwave signature from land surfaces: A review of recent results and application to the L-Band SMOS & SMAP soil moisture retrieval algorithms, Remote Sens. Environ., 192, 238–262, 2017. **(Radiometer)**
- Work, R. A., Stockwell, H. J., Freeman, T. G., and Beaumont, R. T.: Accuracy of field snow surveys, western United States, including Alaska, Cold Regions Research and Engineering Laboratory (U.S.) Technical report, 163, 49 p., <https://hdl.handle.net/11681/5580>. 1965. **(Snow core)**

- Wright, M., Kavanaugh, K., and Labine C.: Performance Analysis of the GMON3 Snow Water Equivalency Sensor. Proceedings of The Western Snow Conference. Stateline, NV, USA, April 2011. Poster on line, <https://www.campbellsci.ca/cs725>, 2011 **(GMON)**
- Wright, M.: CS725 Frozen Potential: The Ability to Predict Snow Water Equivalent is Essential. METEOROLOGICAL TEChnOLOGy InTERnATIOnAL, August 2013, 122-123, <https://www.meteorologicaltechnologyinternational.com>, 2013. **(GMON)**
- Xu, X., Baldi, C., Bleser, J.-W., Lei, Y., Yueh, S., and Esteban-Fernandez, D.: Multi-Frequency Tomography Radar Observations of Snow Stratigraphy at Fraser During SnowEx, in Proceedings of the IGARSS 2018-2018 IEEE International Geoscience and Remote Sensing Symposium, Valencia, Spain, 22–27 July 2018, 2018. **(FMCW-Radar)**
- Yankielun, N., Rosenthal, W., and Robert, D.: Alpine snow depth measurements from aerial FMCW radar. Cold Reg. Sci. Technol., 40, 123–134, 2004. **(FMCW-Radar)**
- Yankielun, N.E., Ferrick, M.G., and Weyrick, P. B.: Development of an airborne millimeter-wave FM-CW radar for mapping river ice, Can. J. Civ. Eng., 20, 1057–1064, 1993. **(FMCW-Radar)**
- Yao, H., Field, T., McConnell, C., Beaton, A., and James A.L.: Comparison of five snow water equivalent estimation methods across categories. Hydrol. Process., 32, 1894–1908, <https://doi.org/10.1002/hyp.13129>, 2018. **(GMON)**